

Expression profiling identifies the CRH/CRH-R1 system as a modulator of neurovascular gene activity

Jan M Deussing¹, Claudia Kühne¹, Benno Pütz¹, Markus Panhuysen¹, Johannes Breu¹, Mary P Stenzel-Poore³, Florian Holsboer¹ and Wolfgang Wurst^{1,2}

¹Max Planck Institute of Psychiatry, Munich, Germany; ²Institute of Developmental Genetics, GSF Research Center for Environment and Health, Munich-Neuherberg, Germany; ³Department of Molecular Microbiology and Immunology, Oregon Health Sciences University, Portland, Oregon, USA

Corticotropin-releasing hormone receptor type 1 (CRH-R1)-deficient mice display reduced anxietylike behavior, a chronic corticosterone deficit, and an impaired neuroendocrine stress response caused by disruption of the hypothalamic-pituitary-adrenocortical (HPA) axis. The molecular substrates and pathways of CRH/CRH-R1-dependent signaling mechanisms underlying the behavioral phenotype as well as the consequences of lifelong glucocorticoid deficit remain largely obscure. To dissect involved neuronal circuitries, we performed comparative expression profiling of brains of CRH-R1 mutant and wild-type mice using our custom made MPIP (Max Planck Institute of Psychiatry) 17k cDNA microarray. Microarray analysis yielded 107 genes showing altered expression levels when comparing CRH-R1 knockout mice with wild-type littermates. A significant proportion of differentially expressed genes was related to control of HPA and hypothalamicpituitary-thyroid (HPT) axes reflecting not only the disturbance of the HPA axis in CRH-R1 mutant mice but also the interplay of both neuroendocrine systems. The spatial analysis of regulated genes revealed a prevalence for genes expressed in the cerebral microvasculature. This phenotype was confirmed by the successful cross-validation of regulated genes in CRH overexpressing mice. Analysis of the cerebral vasculature of CRH-R1 mutant and CRH overexpressing mice revealed alterations of functional rather than structural properties. A direct role of the CRH/CRH-R1 system was supported by demonstrating Crhr1 expression in the adult murine cerebral vasculature. In conclusion, these data suggest a novel, previously unknown role of the CRH/CRH-R1 system in modulating neurovascular gene expression and function.

Journal of Cerebral Blood Flow & Metabolism (2007) 27, 1476-1495; doi:10.1038/sj.jcbfm.9600451; published online 7 February 2007

Keywords: corticotropin-releasing hormone; HPA axis; knockout; microarray; neurovascular; overexpression

Introduction

The neuropeptide corticotropin-releasing hormone (CRH) plays a central role in integrating the neuroendocrine, autonomic, and behavioral responses to stress. To coordinate these tasks, CRH displays a dual capacity acting not only as a secretagogue within the line of the hypothalamicpituitary-adrenocortical (HPA) axis but also as a neurotransmitter modulating synaptic neurotransmission in the central nervous system (Deussing and Wurst, 2005).

Clinical studies, supported by pharmacologic and genetic animal models, have demonstrated a prominent role of CRH in mood and anxiety disorders (Holsboer, 1999; Groenink et al, 2003). Hypersecretion of CRH from the paraventricular nucleus of the hypothalamus accounting for HPA axis hyperactivity as well as elevated CRH levels detectable in the cerebrospinal fluid are prominent findings in patients with major depression (Nemeroff et al, 1984).

As another hypothalamic-pituitary-end organ axis, the hypothalamic-pituitary-thyroid (HPT) axis has been implicated in affective disorders (Musselman and Nemeroff, 1996). The HPA axis has a direct

Correspondence: Dr JM Deussing, Max Planck Institute of Psychiatry, Molecular Neurogenetics, Kraepelinstrasse 2-10, Munich 80804, Germany.

E-mail: deussing@mpipsykl.mpg.de

This work was partially supported by the Bundesministerium für Bildung und Forschung within the framework of the NGFN2 (01GS0481) and by the Fonds der Chemischen Industrie.

Received 7 July 2006; revised 8 December 2006; accepted 13 December 2006; published online 7 February 2007



impact on the HPT axis by inhibiting its function via CRH and glucocorticoids (Tsigos and Chrousos, 2002).

Besides their crucial role in regulating the neuroendocrine and behavioral stress responses, CRH and its receptors (CRH-Rs) affect peripheral cardiovascular function. Central administration of CRH elevates blood pressure and heart rate, whereas peripheral administration of CRH results in vasodilatation and decreased blood pressure (Parkes *et al*, 2001). Thyroid hormones as the end-effectors of the HPT axis also have a pronounced effect on the cardiovascular system, for example, hyperthyroidism results in increased cardiac output, heart rate, pulse and blood pressure, and decreased vascular peripheral resistance (Vargas *et al*, 2006).

In the last decade, numerous constitutive and conditional mouse mutants have been generated to dissect the pathways implicated in HPA system regulation and CRH-related circuitries involved in anxiety- and stress-related behavior in vivo (Muller and Holsboer, 2006). Nevertheless, the molecular mechanisms behind CRH neurocircuitry regulation and its respective impact on aberrant behavior are yet not fully understood. Corticotropin-releasing hormone receptors are G protein-coupled heptahelical transmembrane receptors, which can couple to multiple G-proteins, and thereby are linked to a variety of intracellular signaling pathways (Reul and Holsboer, 2002). Recently, in vivo experiments demonstrated the involvement of mitogen-activated protein kinase signaling pathways that specifically mediate the behavioral adaptation to stress in response to CRH in distinct brain areas (Refojo et al, 2005).

The combination of microarray technology and existing mouse mutants relevant to the CRH/CRH-R system has already proven as a powerful approach to identify entirely new genes involved in adaptive processes evoked by an imbalance of the CRH/CRH-R system as recently demonstrated by Peeters *et al* (2004).

Here we report on the comparative analysis of cerebral gene expression profiles of CRH-R type 1 (CRH-R1) wild-type and knockout mice. We were able to identify alterations in the expression of genes related to the control of HPA and HPT axes. Additionally, the spatial analysis of candidate genes revealed a previously unknown role of the CRH-/CRH-R1 system in control of cerebrovascular gene expression.

Materials and methods

Mice

Corticotropin-releasing hormone receptor type 1 knockout (KO) mice have been described previously (Timpl *et al*, 1998). Male CRH-R1-deficient mice and wild-type littermates were obtained from heterozygous breedings. Mice were genotyped by polymerase chain reaction (PCR) using

primers: R1-GT1, 5'-TCA-CCT-AAG-TCC-AGC-TGA-GGA-3'; R1-GT2, 5'-GTG-CTG-TCC-ATC-TGA-CGA-GA-3'; R1-GT3B, 5'-GGG-GCC-CTG-GTA-GAT-GTA-GT-3'. Standard PCR conditions result in a 697 bp wild-type and a 496 bp mutant PCR product. Mice overexpressing CRH under the control of the metallothionein promotor have been described previously and were kindly provided by Stenzel-Poore $et\ al\ (1992)$. Corticotropin-releasing hormone transgenic mice and wild-type littermates were obtained from breeding of hemizygous males with wild-type C57BL/6J females. Mice were backcrossed for N=18 generations. Transgenic animals were visually distinguished from their wild-type littermates by their severe Cushing-like phenotype.

RNA Extraction

Mice (10 weeks old) were killed by cervical dislocation at 10 am. Brains were carefully removed and immediately transferred into an appropriate volume (1 mL/100 mg) of TRIzol reagent (Invitrogen, Karlsruhe, Germany). Tissue was thoroughly homogenized using an Ultra-Turrax grinder (IKA-Labortechnik, Staufen, Germany) and subsequently total RNA was prepared according to the manufacturer's recommendations. Quality of total RNA was visually inspected by denaturing agarose gel electrophoresis.

Quantitative Northern Blot Analysis

Five micrograms of total brain RNA were separated in a 1% formaldehyde agarose gel, transferred to Porablot NY Plus membrane (Macherey & Nagel, Düren, Germany) and hybridized with respective [α -32P]dCTP-labeled (Megaprime labeling kit, Amersham, Piscataway, USA) cDNA probes. Filters were washed at high stringency as described. Membranes were stripped by boiling in 0.1% SDS for 10 mins and rehybridized with a 540-bp cDNA fragment of murine β -actin. Expression levels were quantified using a FUJIX BAS-3000 Phosphoimager (Fuji, Japan) and TINA 2.09 software (Raytest, Straubenhardt, Germany). The expression levels were normalized by the signal intensity of murine β -actin expression.

Microarray Construction

The MPIP 17k cDNA microarray contained 18856 PCR products derived from different mouse cDNA libraries (sources: Research Genetics, RZPD Deutsches Ressourcenzentrum für Genomforschung, proprietary clones) representing 12037 different unigene clusters (unigene build #144). The spotting buffer contained $3 \times SSC$ (standard sodium citrate) and 1.5 mol/L betaine. The PCR products were spotted on gamma-amino-propylsilane-coated slides (GAPS II, Corning, NY, USA) using a Chipwriter Pro spotting robot (Biorad, München, Germany) and 48 SMP3 stealth pins (TeleChem, Sunnyvale, CA, USA). After spotting, the arrays were heated to 80°C for 10 secs and crosslinked using a UV Stratalinker 2400 at 200 mJ (Stratagene, Cedar Creek, TX, USA). For blocking, arrays



were submerged in a mixture of 1.25 g succinic anhydride/ 250 mL 1,2-dichloroethane/3.1 mL 1-methylimidazole for 1 h at room temperature. Subsequently, arrays were washed in 250 ml fresh dichloroethane, denatured in boiling ultrapure water for 2 mins, rinsed in 95% ethanol, and finally dried by centrifugation for 1 min at 1500 r.p.m. Arrays were stored in a dark, dry box at room temperature until usage.

Microarray Hybridization

We performed a dual color microarray experiment with a direct comparison of directly labeled, total RNA pools including three technical replicates and dye-swap. Briefly, 100 µg of total RNA from each animal were subjected to a labeling reaction using oligo (dT) Primer (Amersham, Piscataway, NJ, USA), Cy3-coupled dUTPs and Cy5coupled dUTPs (Amersham), and SuperScriptII reverse transcriptase (Invitrogen). After purification of labeling reaction using Bio-6-columns (Biorad) and YM-30 columns (Millipore), 100 µg of Cy3- and Cy5-labeled total RNA from wild-type and knockout mice was combined with hybridization buffer, denatured at 95°C for 3 mins, and hybridized to each of the three technical replicates, resulting in a total of six microarrays. The hybridization buffer contained 50% formamide, 50 mmol/L sodium phosphate buffer (pH 7.0), 5 × Denhard's solution (Sigma, Taufkirchen, Germany), $6 \times SSC$, 0.5% SDS, 0.4 mg/mL murine COT1-DNA (Invitrogen), and 5 μg poly(dA) (Amersham). Hybridization was performed in hybridization chambers submerged in a waterbath at 42°C for 16 h. The arrays were washed for 15 mins in $2 \times$ SSC/0.2% SDS at 60° C, in $0.5 \times$ SSC for 15 mins at 60° C, rinsed in 0.2 × SSC for 1 min at room temperature, shaken vigorously in 0.05 × SSC at room temperature, and finally dried with Servisol Air Spray (Roth, Karlsruhe, Germany). All slides were scanned immediately after drying.

Microarray Analysis

Scanning was performed using a ScanArray 4000 laser scanner and ScanArray 3.1 Software (Perkin Elmer, Boston, MA, USA) with a fixed photomultiplier tube gain of 80%, and 98% (Cy3) or 70% (Cy5) laser power. Quantification was performed using QuantArray software 2.1.0.0 (Perkin Elmer Rodgau-Jügesheim, Germany) and the fixed circle-analysis method. Data were imported in a PSQL relational database for further analysis. Raw data were normalized according to the procedure outlined in Yang et al (2002) and subjected to a t-test for significantly differential expression. The obtained P-values were corrected for multiple testing using Benjamini-Hochberg's false discovery rate procedure (Hochberg and Benjamini, 1990). Because we anticipated strong dilutive effects by the whole-brain approach, a low threshold was chosen for selection of candidate genes: |Z-score $| \ge 1.837$ and | fold |regulation $| \ge 1.1$. Additionally, a raw signal intensity ≥1000 was set as threshold ensuring the practicability of independent confirmation by Northern blot or in situ hybridization.

Quantitative *In Situ* Hybridization

Mice (10 weeks old) were killed by an overdose of isoflurane. Brains were carefully removed and immediately shock frozen on dry ice. Frozen brains were cut on a cryostat in 20- μ m-thick sections. Cryostat sections of wildtype and knockout brains were mounted side by side on SuperFrost Plus slides (Menzel GmbH, Braunschweig, Germany). This procedure allowed for parallel in situ hybridization of wild-type and knockout sections under absolutely identical conditions assuring meaningful quantification and comparison of hybridization signals. All sections were processed for in situ hybridization according to a modified version of the procedure described by Dagerlind et al (1992). Specific riboprobes were generated by PCR from respective cDNA clones, which were spotted on the MPIP 17k array. Polymerase chain reaction products were amplified with primers: T3 5'-GCT-AAA-ATT-AAC-CCT-CAC-TAA-AGG-GAA-TAA-GC-3'; T7 5'-CGA-ATT-TAA-TAC-GAC-TCA-CTA-TAG-GGA-ATT-TG-3' universally applicable for pT7T3D-PAC derived plasmids. The following riboprobes were generated: Rgs5 gene (length ~ 1000 bp, GenBank Accession No. AI847151), Sparc (length ~ 1000 bp, GenBank Accession No. AI840232), Sepp1 (length ~1700 bp, GenBank Accession No. AI838693), Pmp22 (length ~1000 bp, GenBank Accession No. AI852430), Vim (length ~685 bp, GenBank Accession No. AI845820), Col1a2 (length ~ 1400 bp, GenBank Accession No. AI838652). Antisense and sense cRNA probes were transcribed from 200 ng of respective PCR product and directly used as a template for the synthesis of radiolabeled transcripts by in vitro transcription with 35S-UTP using T7 and T3 RNA polymerase, respectively. After 20 mins of DNase I (Roche, Penzberg, Germany) treatment, the probes were purified by the RNeasy Clean up protocol (Qiagen, Hilden, Germany) and measured in a scintillation counter. For hybridization, sections were pretreated and prehybridized as described previously (Dagerlind et al, 1992). Subsequently, they were hybridized overnight with a probe concentration of 7×10^6 c.p.m./mL at 57° C and washed at 65° C in $0.1 \times$ SSC and 0.1 mmol/L dithiothreitol. The hybridized slides were dipped in autoradiographic emulsion (type NTB2; Eastman Kodak, Rochester, NY, USA), developed after 3 to 6 weeks, and counterstained with cresyl violet.

Alkaline Phosphatase Cytochemistry

Alkaline phosphatase (AP) is a marker for arteries, arterioles, and capillaries, and distinguishes afferent from efferent blood vessels in the brain. Alkaline phosphatase activity was assessed on $20 \,\mu\mathrm{m}$ cryosections, which were mounted side by side on SuperFrost Plus slides (prepared as described above for in situ hybridization). Staining was performed for 10 mins at room temperature using either nitro blue tetrazolium chloride/5-bromo-4-chloro-3-indolyl phosphate (NBT/BCIP, Roche, Penzberg, Germany) or Vector Red (Vector Laboratories, Burlingame, CA, USA) as an AP substrate. Enzymatic reaction was stopped by washing in phosphate-buffered saline followed by embedding in ProTaq MountFluor (Quartett Immunodiagnostics, Berlin, Germany).



Endogenous AP activity of cerebral blood vessels was visualized in intact brains as follows. Mice were killed by an overdose of isoflurane and transcardially perfused as follows: $30 \sec 50 \text{ U/}\mu\text{L}$ heparin-NaCl 0.9%, $3 \min 4\%$ cold paraformaldehyde and finally with 7.5 ml NBT/BCIP per animal. Brains were immediately removed and transferred into 4% paraformaldehyde. Photographs were taken using a Leica MZ APO binocular.

Immunofluorescence

Immunofluorescence detection of collagen type IV (CO-LIV) was performed on $20 \,\mu m$ cryostat sections, stored at -20°C until used. Sections were warmed for 5 mins at room temperature (RT; incubations were performed at RT unless indicated otherwise), fixed 5 mins in 4% paraformaldehyde, washed 3 × 5 mins in 0.01% Tween/PBS (PBST), blocked 60 mins in 2% BSA (Sigma)/PBST, and washed 3×5 mins in 0.01% PBST. The goat anti-type IV collagen antibody (Southern Biotech, Galveston, TX, USA) was diluted 1:200 in 0.01% PBST and incubated overnight at 4°C. Sections were washed 3×5 mins in PBS and incubated for 60 mins with the donkey anti-goat, biotinylated antibody (Jackson ImmunoResearch, Cambridgeshire, UK), diluted 1:100. Subsequently, sections were washed 3 × 5 mins in PBS and detection was performed incubating for 60 mins with Texas Red Streptavidin (Vector Lab, Burningham, Canada) diluted 1:50 in PBS. Finally, sections were washed 3 × 5 mins in PBS and mounted in ProTaq MountFluor (Quartett Immunodiagnostics, Berlin, Germany). Photographs were taken using a Zeiss axioplan2 microscope.

Preparation of Cerebral Microvessels

Murine brain microvessels were prepared from fresh brain tissue removed within minutes from 10-week-old mice killed by cervical dislocation. The brain was cleared from meninges and large surface vessels and then minced with a scalpel into approximately 1 mm segments. Tissue was homogenized in ice-cold Dulbecco's modified Eagle's medium-nutrient mixture F-12 (DMEM F-12; Invitrogen) and centrifuged at 228g for 5 mins. After removal of the supernatant, the pellet was resuspended in 15 ml of 18% (wt/vol) dextran solution and centrifuged at 12,000g for 10 mins. The supernatant was removed and the pellet was resuspended in 5 ml of Ca²⁺ Mg²⁺ -free Hank balanced salt solution (Invitrogen). The suspension was passed through a $70\,\mu\mathrm{m}$ nylon mesh filter (BD Biosciences, Bedford, MA, USA) and the filter was washed three times with HBBS. Microvessels retained on the filter were dislodged by inverting the filter and rinsing in 1 mL TRIzol per brain. Total RNA from cerebral microvessels was prepared using the TRIzol reagent (Invitrogen, Karlsruhe, Germany) as described for total brain RNA.

RT-PCR Analysis

Expression of Crh, Crhr1, and Crhr2 in cerebral microvessels was analyzed by RT-PCR. First-strand cDNA synthesis from $1\,\mu g$ total microvascular RNA and $1\,\mu g$

total brain RNA was performed with SuperScript™ II reverse transcriptase (Invitrogen), according to the manufacturer's protocol using an oligo (dT) primer. The following intron-spanning primers were used for genespecific PCRs: Crh: forward 5'-CAC-CTA-CCA-AGG-GAG-GAG-AA-3', reverse 5'-GTT-GCT-GTG-AGC-TTG-CTG-AG-3' (amplifying nucleotides 143 to 711 of mouse Crh cDNA, GenBank Accession No. NM 205769, 35 cycles); Crhr1: forward 5'-GCC-GCC-TAC-AAC-TAC-TTC-CA-3', reverse 5'-CAG-AAA-ACA-ATA-GAA-CAC-AGA-CAC-G-3' (amplifying nucleotides 768 to 1289 of mouse Crhr1 cDNA, GenBank Accession No. NM 007762, 35 cycles); Crhr2: forward 5'-ATG-TTT-GTG-GAG-GGC-TGC-TA-3', reverse 5'-GTC-TGC-TTG-ATG-CTG-TGG-AA-3' nucleotides 792 to 1411 of mouse Crhr2 cDNA, GenBank Accession No. NM 009953, 35 cycles); Glut1: forward 5'-CAT-CTT-CGA-GAA-GGC-AGG-TG-3', reverse 5'-CCT-CGG-GTG-TCT-TGT-CAC-TT-3 (amplifying nucleotides 1067 to 1680 of mouse Glut1 cDNA, GenBank Accession No. BC 055340, 25 cycles); Rgs5: forward 5'-GGG-AAT-TCT-CCT-CCA-GAA-GC-3', reverse 5'-AAA-TTC-AGA-GCG-CAC-AAA-GC-3' (amplifying nucleotides 147 to 603 of mouse Rgs5 cDNA, GenBank Accession No. NM 009063, 30 cycles); Actb: forward 5'-ATC-GTG-CGT-GAC-ATC-AAA-GA-3', reverse 5'-ACA-TCT-GCT-GGA-AGG-TGG-AC-3' (amplifying nucleotides 702 to 1146 of mouse Actb cDNA, GenBank Accession No. NM 007393, 25 cycles); Nrgn: forward 5'-GAC-TAG-GCC-AGA-GCT-GAA-CG-3', reverse 5'-TGA-AAA-CCT-CCT-CCC-CTC-TT-3' (amplifying nucleotides 492 to 1,053 of mouse Nrgn cDNA, GenBank Accession No. NM 022029, 25 cycles); microtuble-associated protein 2 (Map2): forward 5'-GGT-CTC-CAG-GGA-TGA-AGT-GA-3', reverse 5'-GTG-TGG-AGG-TGC-CAC-TTT-TT-3' (amplifying nucleotides 5122 to 5540 of mouse Map2 cDNA, GenBank Accession No. XM 901540, 25 cycles); Gfap: forward 5'-GCC-ACC-AGT-AAC-ATG-CAA-GA-3', reverse 5'-CCT-TCT-GAC-ACG-GAT-TTG-GT-3' (amplifying nucleotides 741 to 1210 of mouse Gfap cDNA, GenBank Accession No. NM 010277, 25 cycles). Polymerase chain reaction products were analyzed by agarose gel electrophoresis together with a DNA marker (Smart Ladder, Eurogentec, Brussels, Belgium).

Data Analysis

Autoradiographs of in situ hybridizations or photographs of AP (NBT/BCIP) stained sections were digitized and relative levels of mRNA or AP staining were determined by computer-assisted optical densitometry (ImageJ, http:// rsb.info.nih.gov/ij/). For in situ hybridizations, routinely three different exposure times were applied to assure that the signals to be quantified were in the linear range. The mean of five to eight measurements was taken from each animal (only three measurements for the paraventricular nucleus (PVN)). Data are presented as fold regulation relative to wild-type measurements. In case of AP staining, the mean of 12 measurements per animal was calculated. Data are presented as mean AP staining intensities ± s.e.m. Data analyses were performed on GraphPad Prism 4 (GraphPad Software Inc., San Diego, CA, USA) using a two-tailed *t*-test. P < 0.05 was taken as significant.



Results

Differential Gene Expression in Corticotropinreleasing Hormone Receptor Type 1 Wild-Type and Knockout Mice

To elucidate molecular mechanisms and neuronal networks underlying the behavioral phenotype, we performed expression profiling utilizing our custommade MPIP-17k cDNA microarray. Total RNA samples, harvested from the brains of five CRH-R1 wild-type and knockout animals at 2 months of age, were pooled genotype-wise. Cy3 and Cy5-labeled RNA pools were hybridized simultaneously to six MPIP-17k arrays including dye-swap. Primary data processing yielded 13,395 analyzable spots. Three thousand nine hundred and twenty-one spots were regulated ± 1.1 -fold and among them 129 spots displayed a |Z-score $| \ge 1.837$ (Supplementary Figure 1). Hundred and eleven spots exhibited a mean expression of ≥1000 representing 107 individual, differentially expressed genes (Table 1). Of these genes, 53 were upregulated and 54 genes were downregulated. Differences in expression levels ranged from +1.7 to -1.5-fold with the majority (78%) of candidate genes showing only weak regulation levels of +1.2 to -1.2-fold. With 48 candidates, almost half of the regulated genes are unknown genes represented by expressed sequence tags or RIKEN clones. Categorization of known candidate genes according to available Gene Ontology (Ashburner et al, 2000) annotations revealed three major functional classes: genes related to signal transduction mechanisms (33%), metabolism (17%), and control of cellular organization (14%; Table 1). Distributed within these classes, we found numerous candidate genes directly connected to the endocrine systems of the HPA and the HPT axis as anticipated from CRH-R1 knockout mice. Genes related to the HPA axis include the nuclear receptor subfamily 3, group C, member 1 (Nr3c1, +1.2-fold), the hydroxysteroid 11-beta dehydrogenase 1 (Hsd11b1, +1.3fold), the FK506-binding protein 4 (Fkbp4, +1.1-fold), calreticulin (Calr, +1.2-fold) as well as the telomerase-binding protein p23 (p23, +1.1-fold). We identified the thyroid hormone receptor alpha (Thra, -1.1-fold), the thyroid hormone receptor interactor 12 (Trip12, -1.2-fold), the type II iodothyronine deiodinase (Dio2, +1.5-fold), transthyretin (Ttr, -1.1/-1.2-fold), and prostaglandin D2 synthase (Ptgds, -1.3/-1.4-fold) as regulated candidate genes related to the HPT axis (Supplementary Figure 2).

Validation of Microarray Data by Quantitative Northern Blot Analysis

To independently confirm the obtained expression profiling data, we performed quantitative Northern blot analysis. The quantification was accomplished with total RNA from the entire brain of CRH-R1 wild-type and knockout littermates (n=7). For

confirmation, genes were chosen that reflected not only the complete bandwidth of differential expression but also the broad spectrum of mean expression levels of identified candidate genes (compare Table 1). Hybridization data were quantified by normalization to β -actin. As an internal control, we demonstrated the absence of Crhr1 expression in the mutant mice. The expression levels of candidate genes analyzed showed a perfect correlation to the mean expression levels obtained from the microarray experiment (data not shown) and confirmed the differential expression of candidate genes (Figure 1). The following regulation levels were detected reflecting the differential expression identified by microarray analysis (microarray results are given in parentheses): regulator of G-protein signaling 5 (Rgs5; Figure 1C) + 1.3-fold (+1.2-fold), secreted protein acidic and rich in cysteine (Sparc; Figure 1D) -1.5-fold (-1.3-fold), Ptgds -1.5-fold (-1.3/-1.4-fold; Figure 1E), makorin 2 (Mkrn2; Figure 1F) -1.3-fold (-1.5-fold), Ttr -1.4-fold (-1.2 fold; Figure 1G). Confirmation of expression and regulation levels established quantitative Northern blot analysis as a valid method for evaluation of microarray data obtained from the MPIP-17k array (Figure 1).

Genes Differentially Regulated in Corticotropinreleasing Hormone Receptor Type 1 Knockout Mice are Inversely Regulated in CRH Overexpressing Mice

Mice ubiquitously overexpressing CRH (CRH-tg) display an opposed phenotype compared with CRH-R1 knockout mice. For CRH-tg mice, an increased anxiety-related behavior and HPA axis hyperactivity with the consequence of a Cushing's syndrome-like phenotype has been reported (Stenzel-Poore et al, 1992; van Gaalen et al, 2002). Thus, we intended to cross-validate candidate genes in CRH-tg mice. For confirmation, Northern blot analysis of total RNA from the entire brain of CRH-tg and respective wild-type littermates (n = 7) was performed. Hybridization with a Crh-specific probe demonstrated a 1.95-fold upregulation of Crh in the entire brain of CRH-tg mice (Figure 1B) whereas expression of Crhr1 was not altered (Figure 1A). Rgs5 (-2.1-fold; Figure 1C), Sparc (+1.3-fold; Figure 1D), Ptgds (+1.6-fold; Figure 1E), and Mkrn2 (+1.3fold; Figure 1F) were significantly regulated in CRH-tg mice. The identified regulation was in the opposite direction compared with CRH-R1 knockout mice while the degree of induction or repression of gene expression was in a similar range as observed in CRH-R1 knockout mice. Only Ttr was not significantly regulated in CRH-tg mice (Figure 1G). The diametrical regulation of candidate genes in CRH-tg mice supports a direct influence of the CRH/ CRH-R1 system on the expression of these genes identified by expression profiling in CRH-R1 knockout mice.

Table 1 Genes up- or downregulated in CRH-R1 knockout mice

Spot	Gene symbol	a	Gene name/description	Accession no.	Unigene cluster	Z-score	Fold regulation	Mean expression	Functional category
7402	Col1a1	CV	Procollagen, type I, alpha 1	AI839149	22621	2.6	1.7	1006	Control of cellular organization
726	Dio2	HPT	Deiodinase, iodothyronine, type II	AI324267	21389	2.3	1.5	1640	Metabolism
6943	Col1a2	CV	Procollagen, type I, alpha 2	AI838652	277792	4.5	1.5	1372	Control of cellular organization
5754	Ptn	CV	Pleiotrophin	AI836517	3063	1.9	1.4	17018	Cell growth and maintenance
13387	Ptn	CV	Pleiotrophin	AI850565	3063	2.9	1.4	3032	Cell growth and maintenance
3903	Vim	CV	Vimentin	AI845820	268000	2.6	1.4	3905	Control of cellular organization
13435			RIKEN cDNA 5133400G04 gene	AI850593	36835	3.4	1.4	2115	Unknown
3337			RIKEN cDNA 1500041J02 gene	AI840941	281019	3.6	1.4	1336	Unknown
16029	TT 11.	TTDA	Hypothetical protein 9630027E11	AI850939	40896	2.3	1.3	1135	Unknown
9375	Hsd11b1	HPA	Hydroxysteroid 11-beta dehydrogenase 1	AI847129	28328	3.2	1.3	1003	Metabolism
15252	Pmp22	CV	Peripheral myelin protein	AI852430	1237	2.8	1.3	1872	Cell growth and maintenance
12312	Ly6c		Lymphocyte antigen 6 complex, locus C	AI844280	1583	2.2	1.3	1382	Immune system
13301	Rapgef3		Rap guanine nucleotide exchange factor (GEF) 3	AI850133	24028	2.0	1.3	1994	Signal transduction mechanism
12838			Weak similarity to protein ref: NP_055284.2 (H. sapiens) testes-specific heterogeneous nuclear ribonucleoprotein	AI845029	40155	1.9	1.2	8973	Unknown
3342	Spred1		G-T Sprouty protein with EVH-1 domain 1, related sequence	AI447802	245890	1.9	1.2	3917	Signal transduction mechanism
1187	Glul	CV	Glutamate-ammonia ligase (glutamine synthase)	AI413315	210745	1.9	1.2	10231	Metabolism
7643			EST	AI839323		2.7	1.2	7358	Unknown
10830			Weak similarity to protein ref: NP_037388.1 (H. sapiens) zinc-finger protein 180	AI847594	1504	2.6	1.2	2129	Unknown
91	Glul	CV	Glutamate-ammonia ligase (glutamine synthase)	AI324037	210745	2.2	1.2	11570	Metabolism
9383	Rgs5	CV	Regulator of G-protein signaling 5	AI847151	20954	1.9	1.2	3633	Signal transduction mechanism
31	Cox8a		Cytochrome c oxidase, subunit VIIIa	AI326932	14022	1.8	1.2	9070	Metabolism
969			RIKEN cDNA 2810410P22 gene	AI845892	28972	4.1	1.2	2636	Unknown
698	Car2		Carbonic anhydrase 2	AI841511	1186	2.4	1.2	8348	Metabolism
0727			EST	AI847573		2.1	1.2	16818	Unknown
3422			Weak similarity to protein pir:T09052 (H. sapiens) T09052 hypothetical protein DBCCR1 – human	AI841051	329074	2.1	1.2	4232	Unknown
3024			RIKEN cDNA B230399N07 gene	AI849887	40192	2.4	1.2	4918	Unknown
6367			Mus musculus transcribed sequence	AI851420	41001	2.6	1.2	4273	Unknown
0603			RIKEN cDNA 4933403G14 gene	AI835009	41709	2.5	1.2	1749	Unknown
250	Nr3c1	HPA	Nuclear receptor subfamily 3, group C, member 1	AI447752	129481	2.3	1.2	5281	Transcription
1313	Calr	HPA	Calreticulin	AI848391	1971	3.4	1.2	14148	Transcription
4372	Rps27a		Ribosomal protein S27a	AI853484	180003	2.5	1.2	13600	Protein synthesis
756	F		RIKEN cDNA 1300007B12 gene	AI845685	18230	3.6	1.2	1020	Unknown
828	Tjp1	CV	Tight junction protein 1	AI847817	4342	2.2	1.2	1904	Control of cellular organization
2031	Gabrb3	= •	Gamma-aminobutyric acid (GABA-A) receptor, subunit beta 3	AI849425	8004	2.3	1.2	3397	Signal transduction mechanis
8092	Amotl1	CV	Angiomotin-like 1	AI839055	159552	2.0	1.2	2360	Unknown
3119			RIKEN cDNA 3526402H21 gene	AI837343	306378	2.0	1.2	1476	Unknown



1482

 Table 1
 Continued

Spot	Gene symbol	a	Gene name/description	Accession no.	Unigene cluster	Z-score	Fold regulation	Mean expression	Functional category
12664			EST	AI844422		2.7	1.1	8045	Unknown
7752			Similar to retinoblastoma-binding protein 6 isoform 2; proliferation potential-related protein; RB-binding Q-protein 1	AI841091	41712	1.9	1.1	1659	Unknown
7804	Sec13l1		SEC13-like 1 (S. cerevisiae)	AI839895	29296	1.9	1.1	1807	Transport facilitation
10618	p23	HPA	Telomerase-binding protein p23 (Hsp90 co-chaperone) (progesterone receptor complex p23)	AI847198		2.0	1.1	4064	Signal transduction mechanism
9224	Pdk3		Pyruvate dehydrogenase kinase, isoenzyme 3	AI845462	12775	2.1	1.1	6354	Signal transduction mechanism
10339			cDNA sequence BC060632	AI846678	334807	2.2	1.1	2269	Unknown
11904	Sap30		sin3 associated polypeptide	AI849299	118	1.9	1.1	3398	Transcription
10484			EST	AI847856		5.2	1.1	8598	Unknown
9596			EST	AI843142		2.0	1.1	3781	Unknown
6561	Hmgcs1		3-hydroxy-3-methylglutaryl-coenzyme A synthase 1	AI841574	61526	1.8	1.1	6685	Metabolism
14054			RIKEN cDNA 6720407G21 gene	AI851909	291906	1.9	1.1	3800	Unknown
11366	Fkbp4	HPA	FK506 binding protein 4	AI848455	12758	1.9	1.1	2026	Siganl transduction mechanism
4820	Rpa2		Replication protein A2	AI465248	2870	2.6	1.1	6034	Transcription
7936	Mbp		Myelin basic protein	AI842020	252063	2.3	1.1	1953	Control of cellular organization
5608			RIKEN cDNA 1810006K23 gene	AI836456	41603	2.7	1.1	15829	Unknown
8697	D 04		EST	AI841156	40===	2.7	1.1	7923	Unknown
6024	Rps24		Ribosomal protein S24	AI836712	16775	1.9	1.1	20983	Protein synthesis Unknown
7854 13783			EST RIKEN cDNA 1500009L16 gene	AI839919 AI851749	271188	2.3 1.9	1.1 1.1	2943 1265	Unknown
6536			EST	AI837837	2/1100	1.9	-1.1 -1.1	7891	Unknown
8670			EST	AI841324		3.6	-1.1 -1.1	43175	Unknown
12416			Expressed sequence AW610627	AI844207	27140	2.0	-1.1 -1.1	2995	Unknown
172	Mapk1		Mitogen activated protein kinase 1	AI323600	196581	2.1	-1.1	3800	Signal transduction mechanism
5364	Ube3a		Ubiquitin protein ligase E3A	AI661496	9002	1.9	-1.1	3948	Protein degradation
11950	Rasa3		RAS p21 protein activator 3	AI848749	18517	2.1	-1.1	2861	Signal transduction mechanism
11182	Ttr	HPT	Transthyretin	AI848407	2108	2.1	-1.1	28065	Protein targeting. Sorting and translocation
10690			RIKEN cDNA 6330417K15 gene	AI847460	259539	3.3	-1.1	4916	Unknown
5746	Pura		Purine-rich element binding protein A	AI836331	259715	1.8	-1.1	5247	Transcription
12919	Thra	HPT	Thyroid hormone receptor alpha	AI844656	265917	3.8	-1.1	10200	Transcription
6055	Gabarapl1		GABA(A) receptor-associated protein-like 1	AI835946	14638	2.5	-1.1	5277	Signal transduction mechanism
8635	Prkce		Protein kinase C, epsilon	AI843403	287660	2.1	-1.1	4610	Signal transduction mechanism
8113	Kif5a		Kinesin family member 5A	AI837333	30355	2.2	-1.1	4057	Transport facilitation
9020			DNA segment, Chr 11, Wayne State University 99, expressed	AI843276	261620	1.9	-1.1	4120	Unknown
11396			RIKEN cDNA 1110051M20 gene	AI849568	233541	2.1	-1.1	2867	Unknown
7792	Aldoc		Aldolase 3, C isoform	AI841101	7729	2.2	-1.1	11424	Metabolism
11876	Dncic1		Dynein, cytoplasmic, intermediate chain 1		20893	1.9	-1.1	3197	Control of cellular organization
11289	Btbd11		BTB (POZ) domain containing 11	AI847060	36544	2.0	-1.2	1368	Protein targeting. Sorting and Translocation
5452			RIKEN cDNA 2810401C16 gene	AI835101	40038	3.1	-1.2	1478	Unknown
8627			EST	AI841304		2.4	-1.2	7452	Unknown
6203			EST	AI836107		2.2	-1.2	11149	Unknown

 Table 1
 Continued

Journal of Cerebral Blood Flow & Metabolism (2007) 27, 1476-1495

Spot	Gene symbol	a	Gene name/description	Accession no.	Unigene cluster	Z-score	Fold regulation	Mean expression	Functional category
13906			EST	AI854455		2.3	-1.2	4690	Unknown
9001			RIKEN cDNA 4933409K07 gene	AI846433	75790	1.9	-1.2	2254	Unknown
6046	Trip12	HPT	Thyroid hormone receptor interactor 12	AI835998	209265	2.1	-1.2	1405	Signal transduction mechanism
7194	Tm9sf2		Transmembrane 9 superfamily member 2	AI838784	275191	2.8	-1.2	1884	Protein targeting. Sorting and translocation
6631			RIKEN cDNA 3110040D16 gene	AI837879	248843	2.3	-1.2	1928	Unknown
6500	Ndrg3		N-myc downstream regulated gene 3	AI836631	279256	5.1	-1.2	13199	Cell growth and maintenance
3882			RIKEN cDNA D030028O16 gene	AI451127	259035	2.4	-1.2	7921	Unknown
10440	Ttr	HPT	Transthyretin	AI847846	2108	2.8	-1.2	27028	Protein targeting. Sorting and translocation
7427			Moderate similarity to protein sp:P98179 (H. sapiens) RBM3_HUMAN Putative RNA-binding protein 3	AI838842	352353	2.7	-1.2	4971	Unknown
14068	Aldh1a1		Aldehyde dehydrogenase family 1, subfamily A1	AI851848	4514	3.2	-1.2	1801	Metabolism
12888			EST	AI845055		2.7	-1.2	4143	Unknown
16284			Similar to eukaryotic translation initiation factor 3, subunit 9	AI854624	21671	2.0	-1.2	2110	Unknown
14905	Ghitm		Growth hormone inducible transmembrane protein	AI852695	182912	4.3	-1.2	2491	Singal transduction mechanism
8846	Camk2a		Calcium/calmodulin-dependent protein kinase (CaM kinase) II alpha	AI846625		2.5	-1.2	5868	Singal transduction mechanism
4559	Icos		Inducible T-cell co-stimulator	AI451625	42044	2.4	-1.2	2796	Immune system
7175			RIKEN cDNA C330002I19 gene	AI838914	250641	2.7	-1.2	5466	Unknown
7042	Sepp1	CV	Selenoprotein P, plasma, 1	AI838693	22699	2.3	-1.2	8751	Control of cellular organization
15005			EST	AI853050		2.6	-1.2	3933	Unknown
12911			RIKEN cDNA 5730469M10 gene	AI850090	27227	2.0	-1.2	4689	Unknown
4652			EST	AI464328		2.4	-1.2	1938	Unknown
7322			EST	AI839328		3.5	-1.2	9975	Unknown
9027	Eef1a1		Eukaryotic translation elongation factor 1 alpha 1	AI843451	335315	2.9	-1.2	9107	Protein synthesis
7829			EŜT	AI840273		1.9	-1.3	2035	Unknown
8844	Sparc	CV	Secreted acidic cysteine-rich glycoprotein		291442	2.6	-1.3	6846	Control of cellular organization
7690	Rap2ip		Rap2 interacting protein	AI839996	2560	2.0	-1.3	2178	Signal transduction mechanism
537	Iars		Isoleucine-tRNA synthetase	AI327140	21118	3.1	-1.3	18315	Protein synthesis
12959	Gng7		Guanine nucleotide binding protein (G protein), gamma 7 subunit	AI850107	222496	2.0	-1.3	13583	Signal transduction mechanism
1615			Similar to mKIAA0284 protein	AI425997	23689	2.9	-1.3	1992	Unknown
15419	Ptgds	CV	Prostaglandin D2 synthase 21 kDa (brain)	AI854274	261831	4.1	-1.3	27463	Metabolism
4555	Ü		RIKEN cDNA 1700047I17 gene	AI451616	295715	1.8	-1.3	1281	Unknown
6786	Apbb1		Amyloid beta (A4) precursor protein- binding, family B, member 1	AI840092	38469	2.4	-1.3	4264	Signal transduction mechanism
5959	Sez6l2		Seizure related 6 homolog (mouse)-like 2	AI835902	283926	2.2	-1.3	3160	Signal transduction mechanism
8722	Gstm1		Glutathione S-transferase, mu 1	AI841346	37199	2.3	-1.4	8713	Metabolism
11801	Ptgds	CV	Prostaglandin D2 synthase 21 kDa (brain)	AI849257	291928	2.4	-1.4	18404	Metabolism
7679	Mkrn2		Makorin, ring finger protein, 2	AI839975	101316	2.1	-1.5	8011	Signal transduction mechanism

^aCategorization of genes related to the hypothalamic-pituitary-adrenocortical axis (HPA). The hypothalamic-pituitary-thyroid axis (HPT) or to the cerebral vasculature (CV).



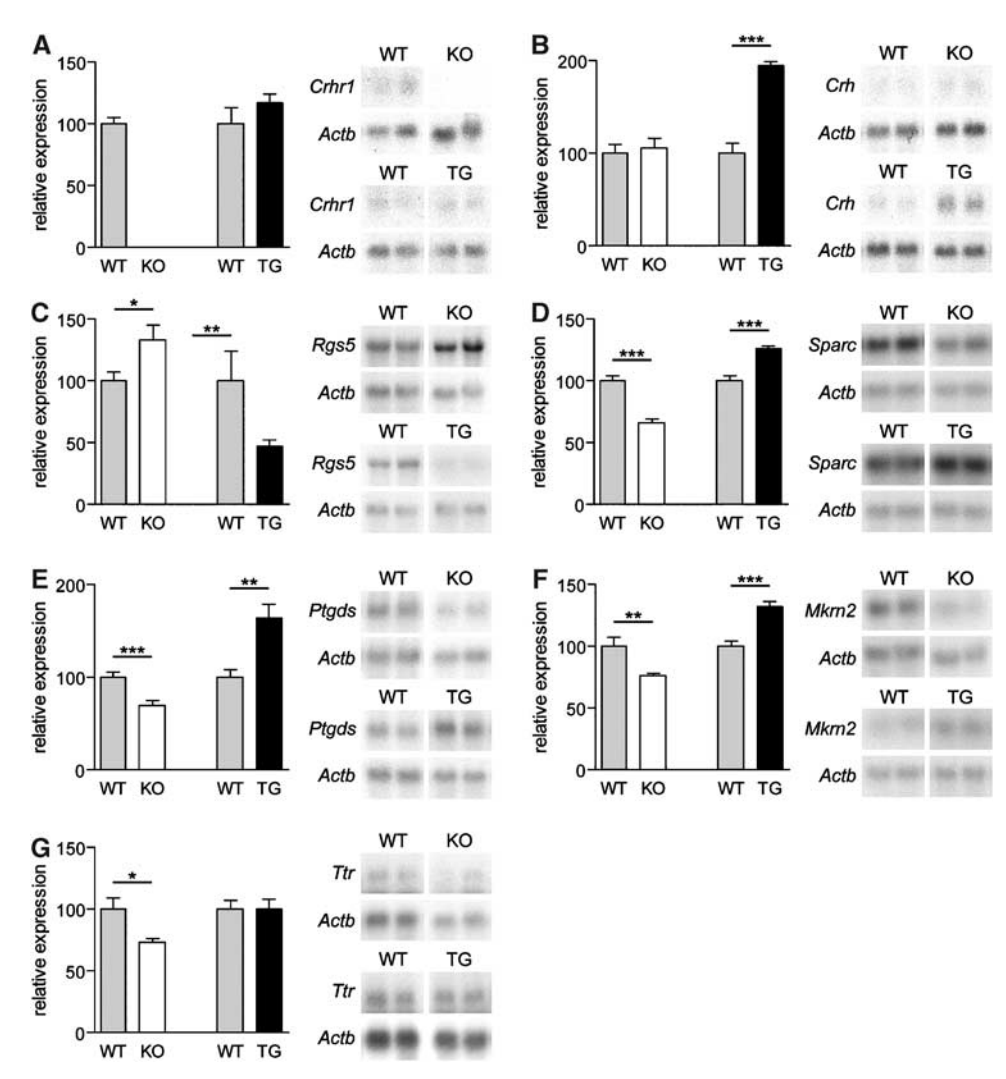


Figure 1 Confirmation of differential expression of selected candidate genes by Northern blot analysis. Validation was performed in CRH-R1 knockout animals and cross-confirmed in CRH-tg animals by comparison with respective wild-type littermates. For quantification, total RNA from the entire brain and scanning densitometry was applied. Relative expression levels were calculated by normalization to β-actin signal intensities. Results are presented as mean ± s.e.m. of seven animals per genotype. Additionally, representative Northern blots are presented for two animals per genotype including β-actin hybridization results. (A) Crhr1 and (B) Crh expression were monitored as internal controls. (C) Rgs5, (D) Sparc, (E) Ptgds, (F) Mkrn2 and (G) Ttr. *P < 0.05, **P < 0.01, ***P < 0.001.

Spatial Analysis of Differentially Expressed Genes by *In Situ* Hybridization

To determine the spatial distribution pattern of candidate genes and to identify those expression domains in the brain causative for the identified changes in gene expression, we performed *in situ* hybridization using riboprobes for selected candidates: Rgs5, Sparc, Ptgds (data not shown), Mkrn2 (data not shown), Ttr (data not shown), peripheral myelin protein 22 (Pmp22), selenoprotein P plasma 1 (Sepp1), vimentin (Vim), and collagen type I alpha 2 (Col1a2). Rgs5 expression was evenly distributed throughout the brain (Figure 2A). Additionally, high levels of expression were detected in the PVN of the hypothalamus (Figure 2B) and in the basolateral

amygdala (Figure 2C). Parallel hybridization of cryosections from wild-type and CRH-R1 mutant brains revealed an overall stronger expression of Rgs5 in CRH-R1 knockout mice (+1.21-fold, P=0.002; two-tailed t-test; Figure 2A). A similar increase in Rgs5 expression was observed in the PVN(+1.27-fold, P < 0.001) whereas expression levels in the basolateral amygdala were not altered (Figures 2B and 2C). Sparc was broadly expressed in the entire brain with highest expression levels in the basal forebrain including septal nuclei, thalamus, hypothalamus, and amygdala as well as throughout the mid- and hindbrain. A significant decrease in expression was observed in septal nuclei located at the ventral midline like in the medial septum (-1.53fold, P=0.001) or the nuclei of the vertical and

horizontal limb diagonal band (Figure 2D). In the PVN of CRH-R1 mutant mice, the expression of Sparc was increased (Figure 2E) whereas the claustrum was identified as a region of diminished Sparc expression in CRH-R1 mutant mice (-1.14-fold, P=0.017; Figure 2F). As already detected for Rgs5, the overall hybridization signal in regions of moderate expression like in the caudate putamen or in the cortex was stronger in CRH-R1 knockout mice as compared with wild-type littermates (+1.21-fold, P=0.001; Figure 2D). The expression of Pmp22 in the mouse CNS has

not been studied in detail, but a recent publication report on the expression of Pmp22 at the developing blood—nerve and blood—brain barriers (Roux et~al, 2004). We found Pmp22 expressed at high levels throughout the brain (Figure 2G). In knockout mice, Pmp22 expression was clearly increased compared with wild-type littermates (+1.17-fold, P<0.001) with strongest differences in the expression observed in the corpus callosum (+1.24-fold, P<0.001) and in the anterior commissure (+1.16-fold, P<0.001; Figures 2H and 2I). In situ hybridization with a

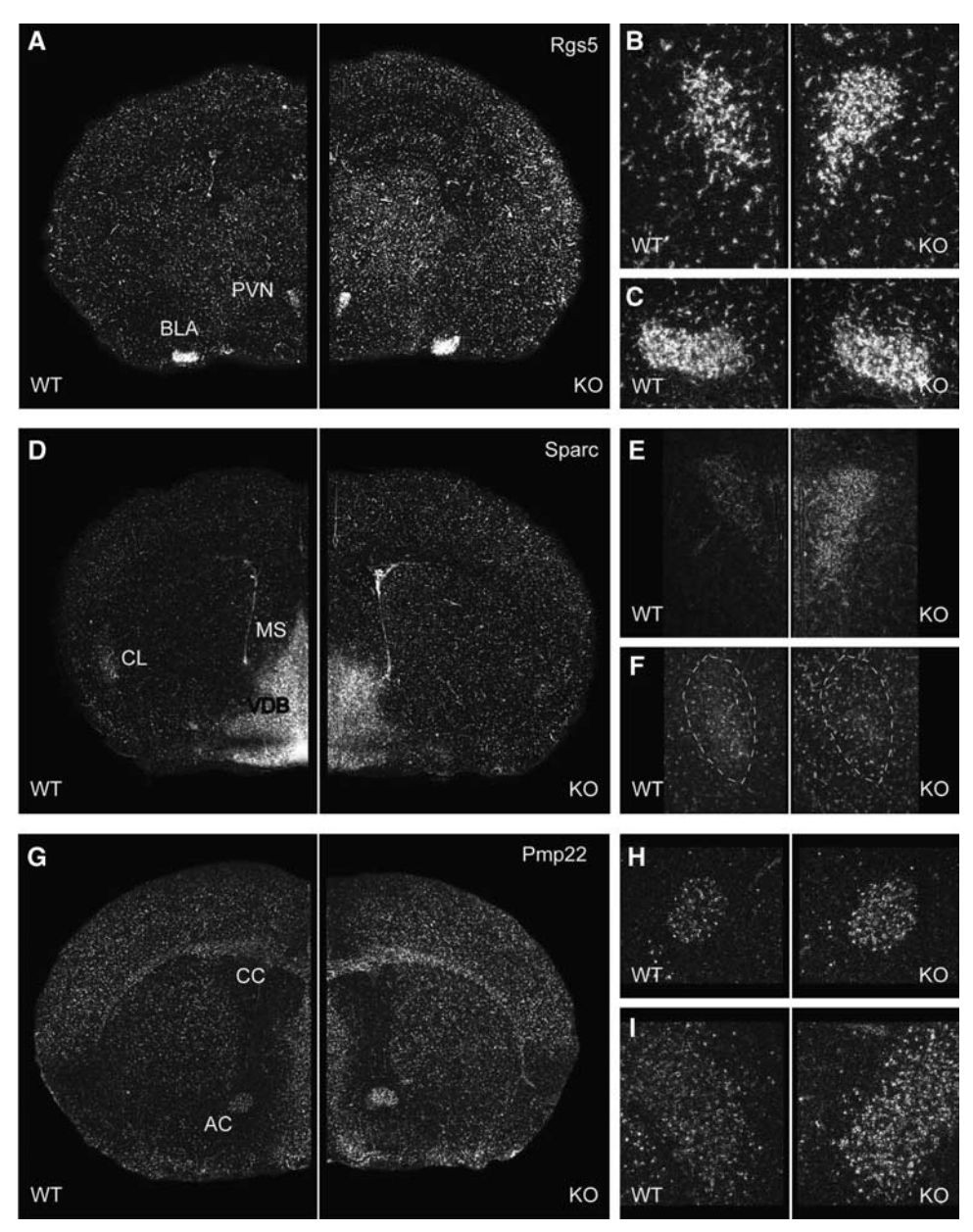


Figure 2 Spatial distribution of selected candidate genes in the adult mouse brain demonstrated by *in situ* hybridization using radiolabeled riboprobes. Each riboprobe was hybridized to sections of 3–5 brains per genotype covering the entire brain from rostral to caudal. Sections of wild-type and CRH-R1 knockout mice were placed side by side on the same slide. Depicted are representative dark field photomicrographs of the coronal sections of Rgs5 (A–C); Sparc (D–F); Pmp22 (G–I); Sepp1 (J, K); Vim (L, M); Col1a2 (N–P). Overviews and close-ups are composed of wild-type (left or top, WT) and knockout (right or bottom, KO) sections. AC: anterior commissure; BLA: basolateral amygdala; CC: corpus callosum; CL: claustrum; MS: nucleus of the medial septum; PVN: paraventricular nucleus; VDB: nucleus of the vertical limb diagonal band.



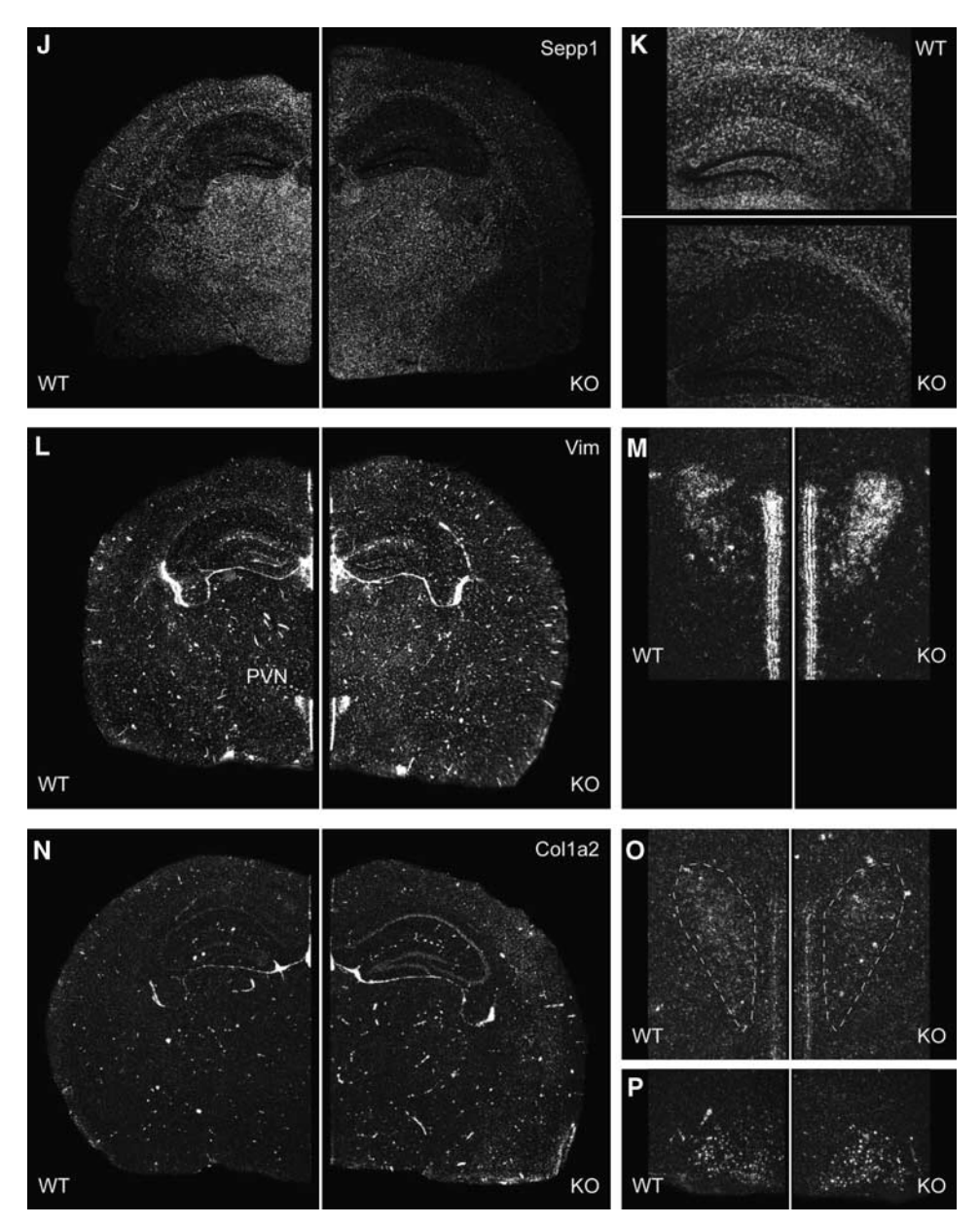


Figure 2 continued

specific riboprobe for Sepp1 demonstrated its ubiquitous expression in the adult murine CNS. Quantification by parallel $in\ situ$ hybridization analysis confirmed the decreased expression of Sepp1 throughout the brain of CRH-R1 knockout mice compared with wild-type littermates (-1.16-fold, P < 0.001; Figure 2J). As for Sparc, the difference in expression was most obvious in the regions of moderate expression like in the hippocampus (Figure 2K). Strong expression of the intermediate filament protein Vim was detected in a scattered pattern throughout the brain, reflecting the cerebral vascular network with blood vessels ranging in diameter from capillaries to arteries and veins. The expression of Vim was markedly increased in CRH-R1 knockout mice compared with wild-type animals

(+1.32-fold; P<0.001; Figure 2L). Additionally, Vim expression was detected in the PVN where its expression was also found to be increased in mutant animals (+1.28-fold, P<0.001; Figure 2M). A comparable but more restricted vascular expression pattern was detected with a specific riboprobe for Col1a2. Col1a2 was predominantly detected in blood vessels of larger diameter, with CRH-R1 knockout mice showing an increased number of Col1a2 positive blood vessels (+1.10-fold, P = 0.032; Figure 2N). Moreover, we identified a previously unrecognized weak expression of Col1a2 in the PVN (Figure 2O) and in the ventromedial hypothalamus (Figure 2P). The expression of Col1a2 in the PVN was downregulated in CRH-R1 knockout mice whereas no difference was observed in the ventromedial hypothalamus.

All genes analyzed by *in situ* hybridization presented a moderate to high expression and were rather ubiquitously dispersed all over the brain. The majority of identified differences in gene expression reflected global changes in expression levels. Nevertheless, some candidate genes exhibited genotypedependent alterations in gene expression that were restricted to specific nuclei and in some cases even showed an opposite regulation compared with observed global changes.

Alterations in Gene Expression in Corticotropinreleasing Hormone Receptor Type 1 Mutant Mice are Predominantly Associated with the Cerebral Vasculature

The majority of genes analyzed by *in situ* hybridization exhibited global changes in activity reflecting

their ubiquitous expression throughout the adult murine brain (Figure 2). A detailed analysis of the spatial distribution pattern of in situ hybridization signals within the brain parenchyma confined the expression not only of Vim and Col1a2 but also of Rgs5, Sparc, and Sepp1 to the neurovascular network (Figures 3D-H). As an example, we demonstrated the microvascular localization of Rgs5. Cells expressing Rgs5 were detected in close vicinity of or attached to arterioles and capillaries as visualized by vector red staining of endogenous AP activity, which is exclusively present in cerebral vascular endothelial cells (Figures 3A-C). Rgs5 and Sparc were clearly upregulated in the cerebral vasculature of CRH-R1 knockout mice as observed for Vim and Col1a2 (Figures 3D, 3E, 3G, and 3H) whereas the expression of Sepp1 was decreased in brain capillaries of mutant animals (Figure 3F). Besides Rgs5, Sparc, Sepp1, Vim, Col1a2, and Pmp22 further

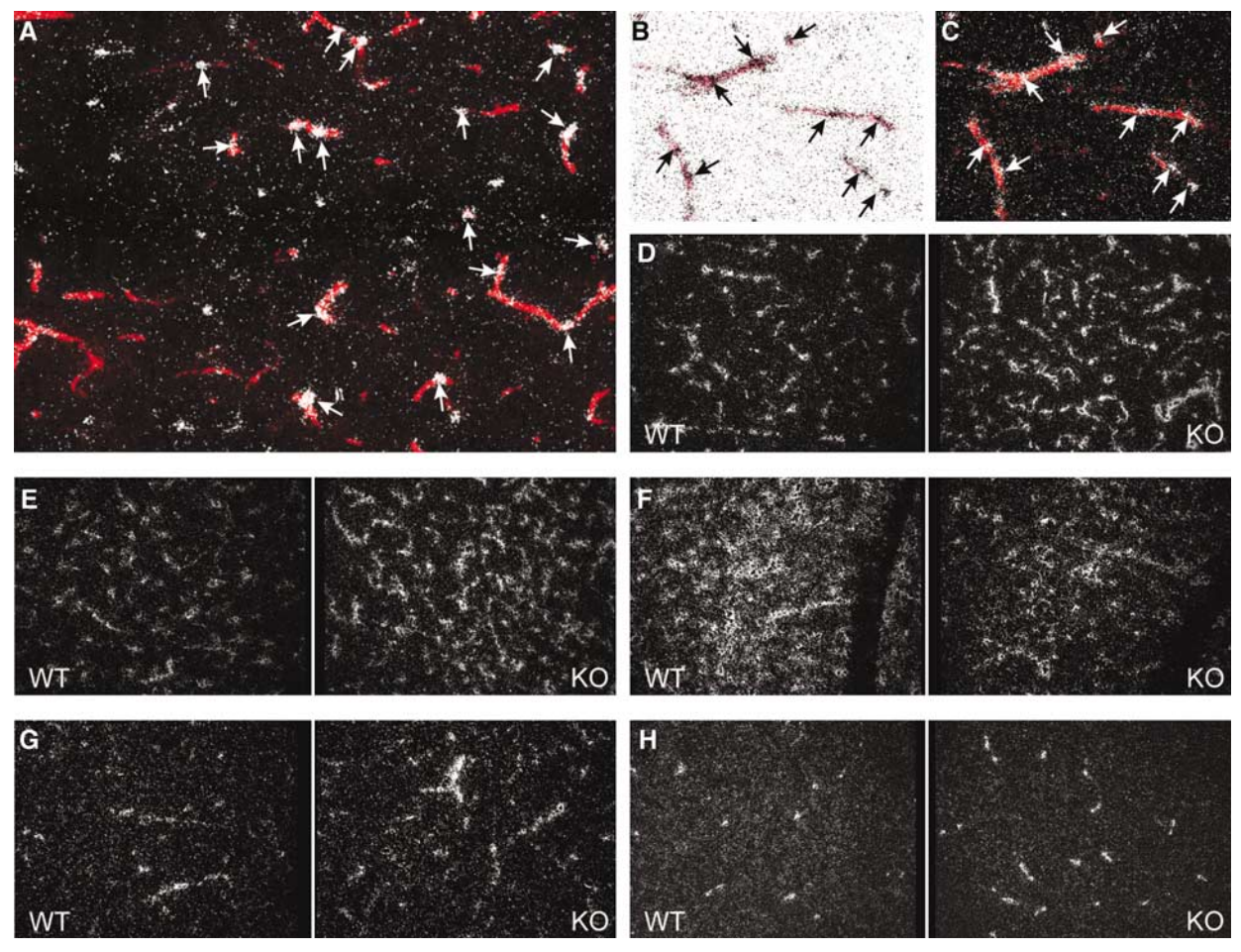


Figure 3 Genes regulated in CRH-R1 knockout mice are differentially expressed within the cerebral vasculature. (A–C) Rgs5 expression was specifically detected in vascular smooth muscle cells and pericytes by *in situ* hybridization and simultaneous AP staining of cerebral blood vessels. (A) Dark field photomicrograph from the cortex displaying Rgs5 expression (arrows) associated with cerebral microvessels (red). (B, C) Bright and respective dark field photomicrograph of brain capillaries with associated Rgs5-expressing pericytes. (D–H) Representative dark field photomicrographs of coronal sections from the cortex hybridized with riboprobes of Rgs5 (D); Sparc (E); Sepp1 (F); Vim (G); and Col1a2 (H). Photomicrographs are composed of wild-type (left, WT) and mutant (right, KO) sections.



genes known to be expressed in cell types associated with the cerebral vasculature were identified among candidate genes obtained by expression profiling: procollagen type I alpha 1 (Col1a1), glutamate-ammonia ligase (Glul), tight junction protein 1 (Tjp1), angiomotin-like 1 (Amotl1), and pleiotrophin (Ptn). In summary, analysis of the spatial expression pattern of candidate genes underscores a predominant effect of the CRH-R1-deficiency on the regulation of genes associated with the cerebral vasculature.

Opposite Regulation of Candidate Genes in Corticotropin-releasing Hormone Overexpressing Mice Confirmed the Changes in Gene Expression Associated with the Cerebral Vasculature

We have demonstrated that genes differentially expressed in CRH-R1 knockout mice were conversely regulated in CRH-tg mice. Therefore, we also examined the expression of genes associated with the cerebral vasculature identified in CRH-R1 knockout mice in the brain of CRH-tg mice (Figure 4). In situ hybridization for Rgs5, Sparc, Sepp1, Vim, and Col1a2 on cryosections of CRH-tg and wild-type control mice confirmed the expression patterns previously observed in CRH-R1 knockout and wild-type mice (Figures 4A–J). While the differences in gene expression restricted to specific brain nuclei were not observed in CRH-tg mice, for example, the expression of Sparc in the claustrum was not altered (Figure 4C), the vascular localization and genotypedependent differential expression was confirmed for all genes analyzed. As observed in the Northern blot analysis, genes upregulated in CRH-R1 mice (Rgs5, Sparc; Vim, Col1a2) were found to be downregulated (Rgs5: -1.57-fold, P < 0.001. Figure 4B; Sparc: Figure 4D; Vim: −1.13-fold, P = 0.023, Figure 4H; and Col1a2: -1.07-fold, P=0.051, Figure 4J) in the cerebral vasculature of CRH-tg mice and vice versa (Sepp: +1.51-fold, P = 0.052; Figure 4F).

The Density of Cerebral Blood Vessels was Affected Neither in Corticotropin-Releasing Hormone Receptor Type 1 Knockout Nor in Corticotropin-Releasing Hormone Overexpressing Mice, but Alkaline Phosphatase Activity was Regulated Differently

To test whether the observed differences in gene expression potentially resulted from quantitative morphologic differences, we investigated the density of the cerebrovascular network. Cryosections of CRH-R1 wild-type and mutant mice were stained for the basement membrane protein collagen IV to visualize blood vessels. No significant genotype-dependent differences regarding the density of capillaries were observed (data not shown). We further examined AP activity, which is a specific marker for endothelial cells of arteries, arterioles,

and capillaries, and distinguishes afferent from efferent blood vessels in the brain (Bell and Scarrow, 1984). Staining of cryosections with the AP substrate BCIP confirmed the similarity of cerebral microvessel density in the brains of CRH-R1 mutant and wild-type animals. However, a strong difference in enzymatic activity became apparent (Figure 5A). Histomorphometrical quantification revealed a 1.8fold upregulation of AP activity in sections of CRH-R1-deficient brains compared with wild-type brains (Figure 5C). Accordingly, collagen IV staining of cerebral blood vessels of CRH-tg mice revealed no genotype-dependent differences in the density of the neurovascular network compared with wildtype littermates (data not shown). However, AP staining manifested a marked decrease of enzymatic activity in CRH-tg brains compared with wild-type littermates (Figures 5B and 5C).

Perfusion of entire brains of CRH-R1 mutant mice and wild-type littermates with BCIP revealed that the increase in AP staining is consistently present throughout the afferent blood supply, from pial arteries on the surface of the brain to intracerebral capillaries (Figures 6A and 6B). This is in contrast to CRH-tg mice, where AP activity is severely downregulated within the afferent blood supply (Figures 6C and 6D). In summary, these results establish AP as a marker reflecting CRH/CRH-R1-dependent changes in neurovascular gene expression.

Corticotropin-Releasing Hormone Receptor Type 1 is Expressed in the Cerebral Microvasculature

The observed changes in cerebrovascular gene expression in CRH-R1 mutant animals and their confirmation in CRH-tg mice suggest a direct role of the CRH/CRH-R system in modulating neurovascular gene expression. Since the expression of CRH and its receptors in the cerebral vasculature of the mouse has not been studied in detail, we investigated the expression of Crh, Crhr1, and Crhr2 by semiquantitative RT-PCR in RNA extracted from specimen enriched in murine cerebral vasculature.

We demonstrated the strong enrichment of cerebral blood vessels using glucose transporter 1 (Glut1) and Rgs5 as specific markers for endothelial and perivascular cells (pericytes and smooth muscle cells), respectively (Figure 7A). The purity of blood vessels was assessed by RT-PCR using neurogranin (Ngrn) as a marker for neurons as well as the Map2, which is a marker for neurons and astrocytes. The low expression of Nrgn in the vascular sample indicates only a minor contamination with neurons. However, the increased expression of Map2 in the vascular sample compared with the brain sample suggests a co-purification of astrocytes that most likely remain attached to the cerebral vasculature. This interpretation is supported by the increased

expression of Gfap observed in the sample enriched in cerebral vasculature (Figure 7A). RT-PCR revealed the expression of Crhr1 in the cerebral vasculature. Crhr2 was also found expressed, however, at lower levels whereas Crh is not expressed or its expression level was below the detection limit (Figure 7B).

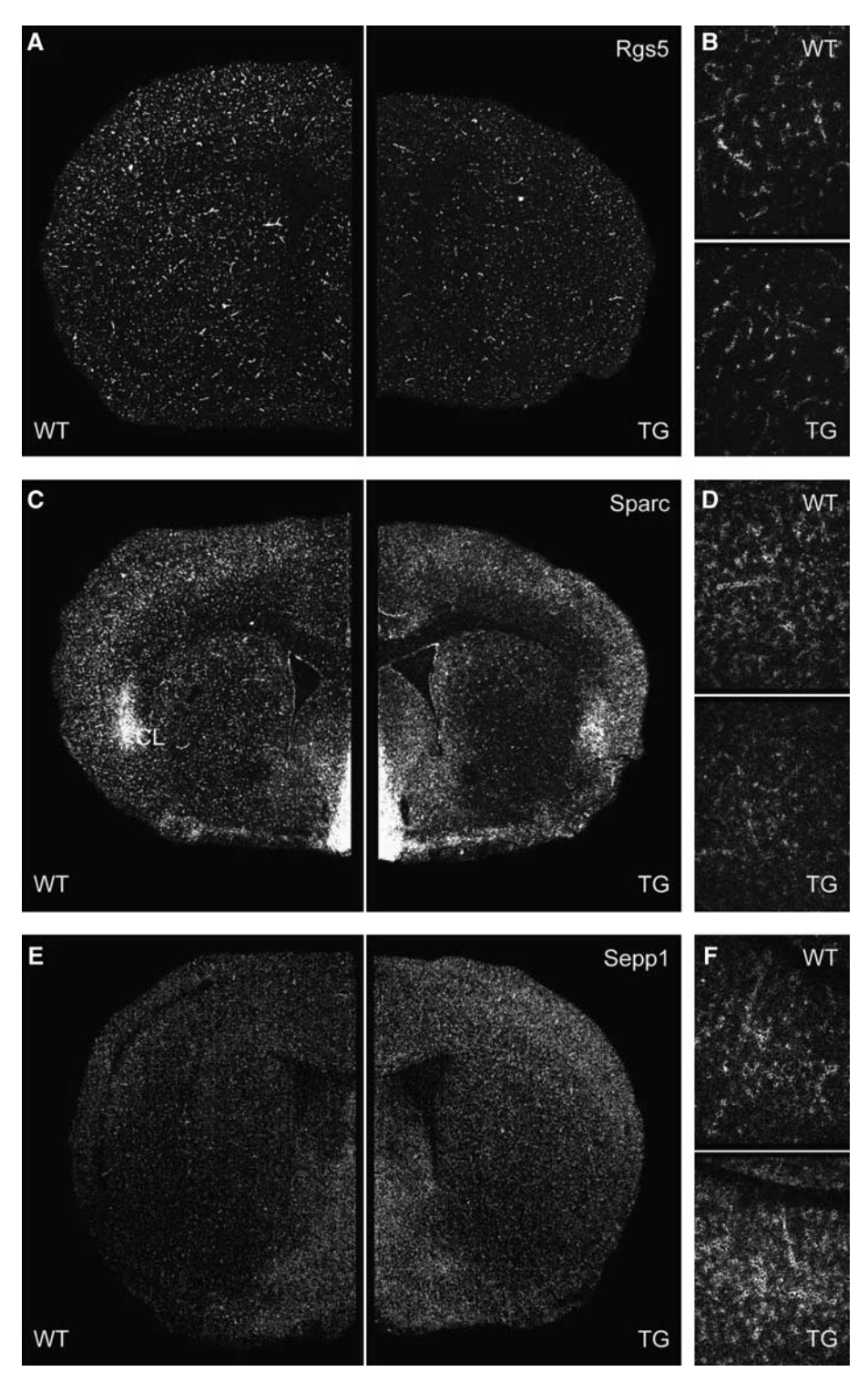


Figure 4 Cross-confirmation of CRH-R1 deficiency-dependent gene expression in the cerebral vasculature of CRH-tg mice. Expression of Rgs5 (**A, B**), Sparc (**C, D**), Sepp1 (**E, F**), Vim (**G, H**), Col1a2 (**I, J**) in adult mouse brains demonstrated by *in situ* hybridization using radiolabeled riboprobes. Each riboprobe was hybridized to sections of 3–5 brains per genotype covering the entire brain from rostral to caudal. Sections of wild-type and CRH-tg mice were placed side by side on the same slide. Representative dark field photomicrographs depict overviews and close-ups of coronal views composed of wild-type (left or top, WT) and CRH-tg (right or bottom, TG) sections.



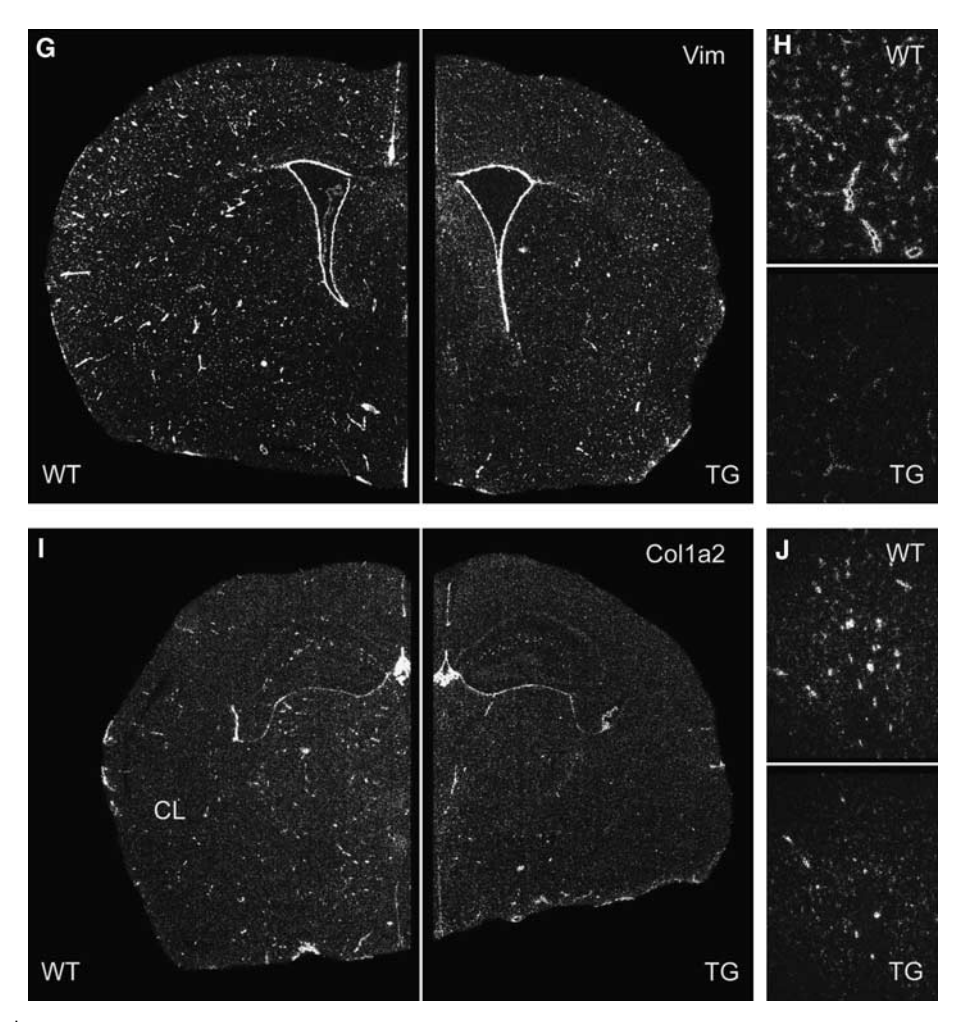


Figure 4 continued

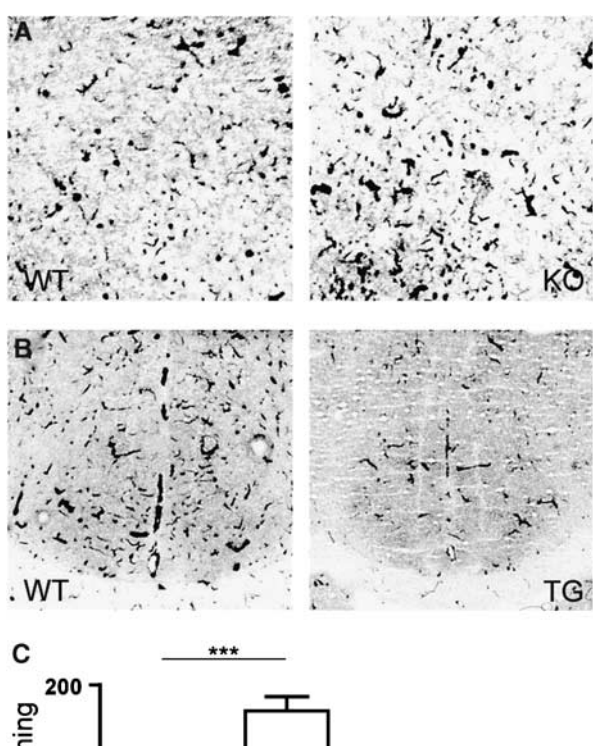
Discussion

Despite the enormous heterogeneity of the brain, which consists of a multitude of different cell types and is composed of numerous functionally and morphologically distinguishable units, we identified and confirmed differentially expressed genes establishing the MPIP-17k array as a reliable platform for expression profiling. The comparison of gene expression profiles of brains derived from CRH-R1 knockout and wild-type mice identified alterations in gene expression predominantly related to (i) the HPA axis, (ii) the HPT axis, and (iii) the cerebral vasculature.

Hypothalamic-Pituitary-Adrenal Axis Dysregulation in Corticotropin-Releasing Hormone Receptor Type 1 Mutant Mice Results in Altered Expression of Genes Controlling Hypothalamic-Pituitary-Adrenal Axis Activity and Glucocorticoid Signaling

The PVN plays a crucial role in controlling HPA axis activity via stress-induced expression and release of

CRH. Disruption of the HPA axis in CRH-R1 knockout mice results in an activation of the hypothalamic vassopressinergic system, which is sufficient to maintain normal basal plasma ACTH levels (Muller et al, 2000). Similar adaptive mechanisms may account for altered expression of Rgs5, Vim, Sparc, and Col1a2 observed in the PVN of CRH-R1 knockout mice. As genes directly related to HPA axis control and glucocorticoid signaling, we found Nr3c1, Hsd11b1, Fkbp4, Calr, and p23 differentially expressed between wild-type and knockout mice. Nr3c1, also known as glucocorticoid receptor (GR), was found to be upregulated 1.2-fold in the brain of CRH-R1 mutant mice. An autoregulation of GR has been demonstrated earlier in adrenal ectomized rats, which show increased hippocampal GR expression (Reul et al, 1989). Hsd11b1, the key enzyme regulating intracellular regeneration of glucocorticoids in the brain and pituitary, was increased 1.3fold in CRH-R1 mutant brains likely by similar regulatory mechanisms. Studies with mice deficient in Hsd11b1 have demonstrated the importance of this 11-β-hydroxysteroid dehydrogenase for HPA axis regulation (Harris et al, 2001). Our result is in



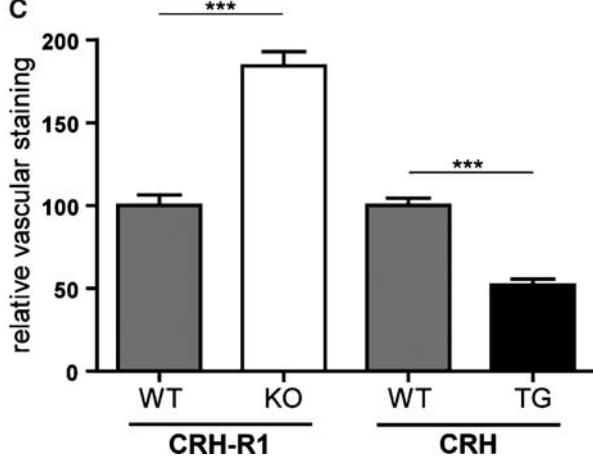


Figure 5 The activity of AP in the cerebral vasculature is altered in CRH-R1 knockout and CRH-tg mice. Representative bright field photomicrographs of AP-stained cryosections from the striatum of (A) CRH-R1 knockout and from the cortex of (B) CRH-tg animals and respective control littermates. (C) Histomorphometric quantification of AP activity on adult brain sections from CRH-R1 knockout and CRH-tg animals.

line with expression-profiling experiments using CRH-tg mice, which reported a 0.57-fold down-regulation of Hsd11b1 in the hippocampus potentially attributed to the chronic elevation of glucocorticoids in these mice (Peeters et al, 2004). Peeters and co-workers further demonstrated a 2.17-fold upregulation of Fkbp5 in the temporal area and in the nucleus accumbens of CRH-tg mice. Our studies revealed an increase of Fkbp4 (+1.1-fold) in the entire brain of CRH-R1 knockout mice. Glucocorticoid receptor forms a heteromultimeric cytoplasmic complex with heat-shock protein (HSP) 90, HSP70, and FKBP5. On ligand binding, FKBP5 is replaced by FKBP4, which links the complex to

dynein and thereby mediates the transport to the nucleus. Expression of p23, another co-chaperone stabilizing the GR-HSP90 complex and involved in GR activation, was found 1.1-fold increased (Dittmar et al, 1997). The upregulation of Calr (+1.2-fold)most likely parallels regulatory mechanisms involving Fkpb4 and p23. CALR is a multifunctional protein, which is capable of binding to the DNAbinding domain of GR and facilitates its export from the nucleus to the cytoplasm (Holaska et al, 2002). In CRH-R1-deficient mice, the increase in Fkbp4, p23, and Calr expression might contribute to compensatory processes counteracting low plasma corticosterone levels, in contrast to CRH-tg mice, where upregulation of Fkbp5 is rather attenuating GR as a response to high levels of circulating glucocorticoids.

Differential Expression of Hypothalamic-Pituitary-Thyroid Axis Components Reflects Cross-Regulatory Mechanisms Between Hypothalamic-Pituitary-Adrenal and Hypothalamic-Pituitary-Thyroid Axes

The HPT axis is a stress-responsive endocrine system, which is regulated by glucocorticoids, the end product of the HPA axis. Different from the HPA axis, the HPT axis is inhibited in depressed patients (Musselman and Nemeroff, 1996). Glucocorticoids repress the HPT axis on the level of the hypothalamus by inhibiting thyrotropin-releasing hormone expression (Kakucska et al, 1995). Activation of the HPA axis has been associated with the decreased production of thyroid-stimulating hormone and inhibition of peripheral conversion of L-thyroxine (T4) to the biologically more active 3,5,3'-L-triiodothyronine (T3). The herein reported microarray analysis identified an altered expression of several major HPT axis components in the brain of CRH-R1 mutant mice reflecting the regulatory influence of the HPA axis. For instance, Ttr (also known as prealbumin), which is in the brain the only thyroid hormone-binding plasma protein, was downregulated 1.1/1.2-fold. Under physiologic conditions, TTR functions as a carrier for T4 and vitamin A, in the latter case through binding to the retinol-binding protein (Monaco, 2000). T4, which is the major secretory product of the thyroid gland, is converted by DIO2 to active T3. Thereby DIO2 plays a critical role in locally regulating the intracellular T3 concentration (Bianco et al, 2002). We found Dio2 upregulated 1.5-fold in mutant mice, potentially resulting in increased brain T3 levels. This result is in agreement with array data by Peeters et al (2004), where Dio2 was found to be downregulated (0.53fold) in the prefrontal cortex of CRH-tg mice. The downregulation of the nuclear hormone receptor Thra (-1.1-fold), which is the executer of T3 activity (O'Shea and Williams, 2002), might reflect a consequence of increased local T3 levels because of elevated DIO2 activity. Finally, the downregulation

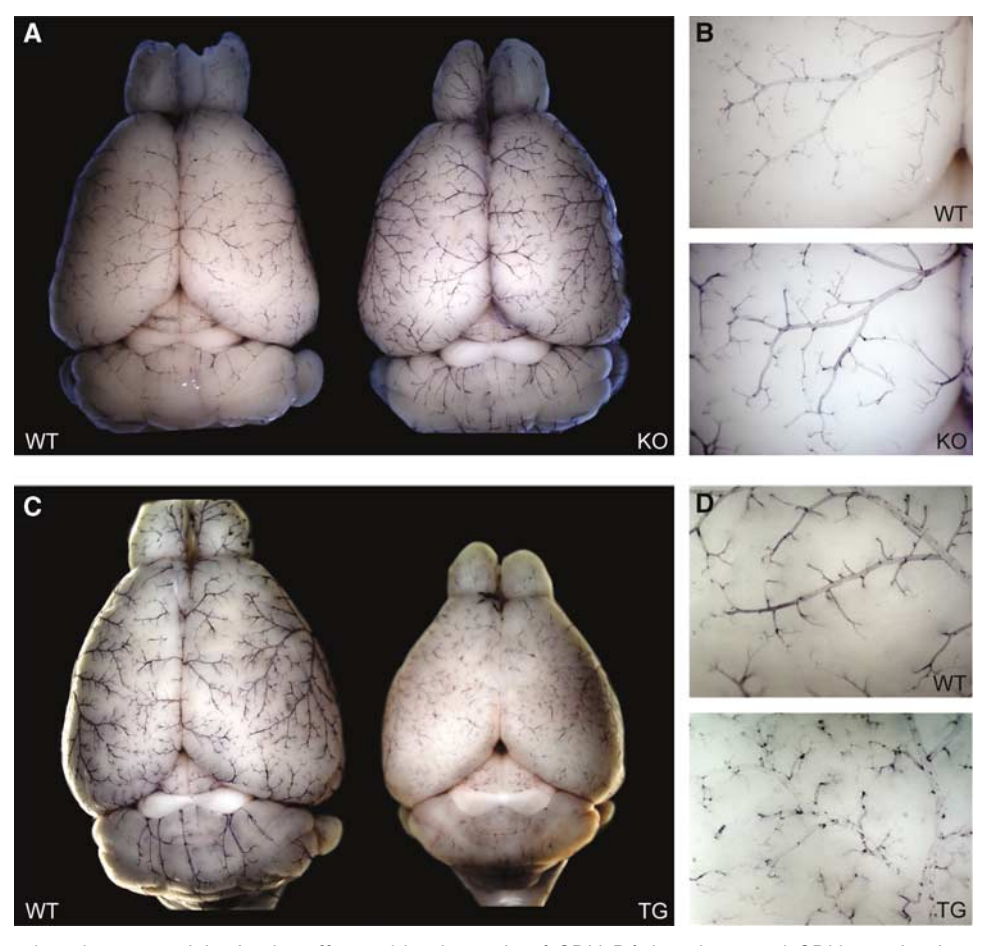


Figure 6 Alkaline phosphatase activity in the afferent blood supply of CRH-R1 knockout and CRH-tg mice is regulated genotype dependently. Dorsal view of (A) CRH-R1 knockout (KO) and (C) CRH-tg (TG) brains and respective wild-type controls (WT, left) after perfusion with the AP substrate NBT/BCIP. (B) Alkaline phosphatase activity in cerebral arteries of CRH-R1 knockout (bottom, KO) animals is increased compared with wild-type animals (WT, top). (D) Alkaline phosphatase activity in cerebral arteries of CRH-tg animals (bottom, TG) is decreased compared with wild-type animals (WT, top).

of Trip12 (-1.2-fold) underscores the direct impact of the HPA axis disruption on the HPT axis in CRH-R1-deficient mice.

Corticotropin-Releasing Hormone Receptor Type 1 **Deficiency and Corticotropin-Releasing Hormone** Overexpression Interfere with Neurovascular Gene **Expression**

Apart from the HPA and HPT axis, our attention was drawn to the cerebral vasculature by the high proportion of regulated genes localized to the microvasculature and to cells associated with the blood-brain barrier. For instance, Rgs5 (+1.2-fold) is almost exclusively expressed throughout the cerebral microvascular network. RGS5 belongs to a large family of multifunctional signaling proteins, acting as GTPase-activating proteins, thereby negatively regulating G protein-coupled receptor signaling. RGS5 was identified as a novel marker for pericytes and vascular smooth muscle cells by the expression profiling of PDGF-B-deficient mouse embryos (Bondiers et al. 2003), and was found downregulated in brain capillaries of stroke-prone spontaneously hypertensive rats (Kirsch et al, 2001). RGS5 regulates platelet-derived growth factor receptor- β and G protein-coupled receptor-mediated signaling pathways active during fetal vascular maturation as well as during phases of active vessel remodeling (Berger et al, 2005).

The expression of several structural constituents of the cerebral vasculature including Sparc, Vim, and Col1a2 was induced in CRH-R1 knockout brains. The Ca²⁺-binding matricellular glycoprotein SPARC modulates the interaction of cells with the extracellular matrix by regulating cell adhesion and binding of growth factors. SPARC regulates the activity of PDGF, VEGF, and fibroblast growth factor-2, which are important for vascular homeostasis (Raines et al, 1992; Kupprion et al, 1998). SPARC was induced in mature blood vessels close to

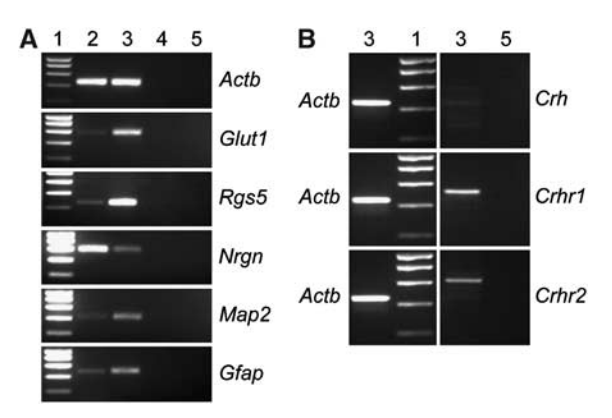


Figure 7 Expression analysis of Crh, Crhr1, and Crhr2 in adult cerebral vasculature. (A) Determination of enrichment of cerebral microvasculature by semiquantitative RT-PCR using markers for: neurons (neurogranin, Nrgn), astrocytes (glial acidic filament protein, Gfap), neurons, and astrocytes (microtubule-associated protein 2, Map2), endothelial cells (glucose transporter 1, Glut1) as well as for pericytes and smooth muscle cells (regulator of G-protein signaling 5, Rgs5). The RT-PCR for β-actin (Actb) demonstrates the utilization of identical amounts of cDNA derived from brain and cerebral vasculature RNA. (B) Expression of Crh, Crhr1, and Crhr2 in specimen enriched in adult cerebral vasculature as determined by RT-PCR. Identity of lanes: lane 1, DNA marker; 2: RT-PCR of total brain RNA; lane 3: RT-PCR of RNA from specimen enriched in cerebral blood vessels; lane 4, no RT control of total brain RNA; lane 5, no RT control of RNA from specimen enriched in cerebral blood vessels.

cerebral lesions suggesting a role in processes related to angiogenesis after injury (Mendis et al, 1998). It is known to bind collagen type I in vivo, which is one of the major fibril-forming extracellular matrix proteins maintaining the structural integrity of blood vessels. SPARC has been shown to suppress the expression of collagen type I (Francki et al, 1999) and a deficiency in type I collagen negatively affects the accumulation of extracellular SPARC (Iruela-Arispe et al, 1996). Type I collagen is a triplestranded rope-like coiled structure of one alpha 2 and two alpha 1 chains. Accordingly we found Col1a2 and Col1a1 upregulated in CRH-R1 mutant brains. Another structural component that was increased in CRH-R1 mutant animals is Vim, an intermediate filament protein found in ependymal cells, and activated astrocytes, but also in cells of blood vessels such as pericytes and smooth muscle cells (Schnitzer et al, 1981).

In contrast to CRH-R2-deficient mice, which develop a systemic hypervascularization postnatally (Bale *et al*, 2002), we could not detect any signs of altered vascular densities in the brain of CRH-R1-deficient mice. This finding rather favors a functional than a structural alteration of the vascular network. This viewpoint is supported by significantly increased AP activity in the afferent cerebral vasculature of CRH-R1 mutant mice, in particular, when considering that the appearance of cytochemi-

cally detectable AP activity in endothelial cells of capillaries and arterioles in mouse brain coincides with maturation of blood-brain barrier (Vorbrodt et al, 1986). The implication of CRH and related peptides in cardiovascular function is well established and may play an important role in cardiovascular adaptations to stress (Coste et al, 2002). Acute stress increases blood-brain barrier permeability, an effect involving CRH, which has been demonstrated to directly affect brain microvessel endothelial cells (Esposito et al, 2002). The expression of CRH receptors in the cerebral vasculature has not yet been studied in detail although the CRH receptor protein has been detected in bovine and rat brain microvascular endothelial cells by Western blot albeit using an antibody detecting both receptors (Esposito et al, 2003). To our knowledge, the present study provides the first evidence by means of RT-PCR that Crhr1 is expressed in the cerebral microvasculature. Whether Crhr1 is expressed in vascular endothelial cells, pericytes, or vascular smooth muscle cells remains to be investigated in detail. Expression in blood vessel-associated astrocytes has been demonstrated recently (Stevens et al, 2003).

Taken together, our data show the potential of microarray analyses not only to dissect the molecular mechanisms underlying known phenotypes but also to identify previously unrecognized phenotypes in genetically engineered mouse models.

Acknowledgements

The authors thank Daniela Kohl, Katja Mayer, Sabrina Meyr, and Tanja Orschmann for excellent technical assistance. We thank Daniela Vogt Weisenhorn, Peter Weber, and Carola Hetzel for helpful contributions.

References

Ashburner M, Ball CA, Blake JA, Botstein D, Butler H, Cherry JM, Davis AP, Dolinski K, Dwight SS, Eppig JT, Harris MA, Hill DP, Issel-Tarver L, Kasarskis A, Lewis S, Matese JC, Richardson JE, Ringwald M, Rubin GM, Sherlock G (2000) Gene ontology: tool for the unification of biology. The Gene Ontology Consortium. *Nat Genet* 25:25–9

Bale TL, Giordano FJ, Hickey RP, Huang Y, Nath AK, Peterson KL, Vale WW, Lee KF (2002) Corticotropinreleasing factor receptor 2 is a tonic suppressor of vascularization. *Proc Natl Acad Sci USA* 99:7734–9

Bell MA, Scarrow WG (1984) Staining for microvascular alkaline phosphatase in thick celloidin sections of nervous tissue: morphometric and pathological applications. *Microvasc Res* 27:189–203

Berger M, Bergers G, Arnold B, Hammerling GJ, Ganss R (2005) Regulator of G-protein signaling-5 induction in pericytes coincides with active vessel remodeling during neovascularization. *Blood* 105:1094–101



- Bianco AC, Salvatore D, Gereben B, Berry MJ, Larsen PR (2002) Biochemistry, cellular and molecular biology, and physiological roles of the iodothyronine selenodeiodinases. *Endocr Rev* 23:38–89
- Bondjers C, Kalen M, Hellstrom M, Scheidl SJ, Abramsson A, Renner O, Lindahl P, Cho H, Kehrl J, Betsholtz C (2003) Transcription profiling of platelet-derived growth factor-B-deficient mouse embryos identifies RGS5 as a novel marker for pericytes and vascular smooth muscle cells. *Am J Pathol* 162:721–9
- Coste SC, Quintos RF, Stenzel-Poore MP (2002) Corticotropin-releasing hormone-related peptides and receptors: emergent regulators of cardiovascular adaptations to stress. *Trends Cardiovasc Med* 12:176–82
- Dagerlind A, Friberg K, Bean AJ, Hokfelt T (1992) Sensitive mRNA detection using unfixed tissue: combined radioactive and non-radioactive *in situ* hybridization histochemistry. *Histochemistry* 98:39–49
- Deussing JM, Wurst W (2005) Dissecting the genetic effect of the CRH system on anxiety and stress-related behaviour. C R Biol 328:199-212
- Dittmar KD, Demady DR, Stancato LF, Krishna P, Pratt WB (1997) Folding of the glucocorticoid receptor by the heat shock protein (hsp) 90-based chaperone machinery. The role of p23 is to stabilize receptor.hsp90 heterocomplexes formed by hsp90.p60.hsp70. *J Biol Chem* 272:21213–20
- Esposito P, Basu S, Letourneau R, Jacobson S, Theoharides TC (2003) Corticotropin-releasing factor (CRF) can directly affect brain microvessel endothelial cells. Brain Res 968:192–8
- Esposito P, Chandler N, Kandere K, Basu S, Jacobson S, Connolly R, Tutor D, Theoharides TC (2002) Corticotropin-releasing hormone and brain mast cells regulate blood–brain-barrier permeability induced by acute stress. *J Pharmacol Exp Ther* 303:1061–6
- Francki A, Bradshaw AD, Bassuk JA, Howe CC, Couser WG, Sage EH (1999) SPARC regulates the expression of collagen type I and transforming growth factor-beta1 in mesangial cells. *J Biol Chem* 274:32145–52
- Groenink L, Pattij T, De JR, van der GJ, Oosting RS, Dirks A, Olivier B (2003) 5-HT1A receptor knockout mice and mice overexpressing corticotropin-releasing hormone in models of anxiety. *Eur J Pharmacol* 463:185–97
- Harris HJ, Kotelevtsev Y, Mullins JJ, Seckl JR, Holmes MC (2001) Intracellular regeneration of glucocorticoids by 11beta-hydroxysteroid dehydrogenase (11beta-HSD)-1 plays a key role in regulation of the hypothalamic-pituitary-adrenal axis: analysis of 11beta-HSD-1-deficient mice. *Endocrinology* 142:114–20
- Hochberg Y, Benjamini Y (1990) More powerful procedures for multiple significance testing. Stat Med 9: 811–8
- Holaska JM, Black BE, Rastinejad F, Paschal BM (2002) Ca2+-dependent nuclear export mediated by calreticulin. *Mol Cell Biol* 22:6286–97
- Holsboer F (1999) The rationale for corticotropin-releasing hormone receptor (CRH-R) antagonists to treat depression and anxiety. *J Psychiatr Res* 33:181–214
- Iruela-Arispe ML, Vernon RB, Wu H, Jaenisch R, Sage EH (1996) Type I collagen-deficient Mov-13 mice do not retain SPARC in the extracellular matrix: implications for fibroblast function. *Dev Dyn* 207:171–83
- Kakucska I, Qi Y, Lechan RM (1995) Changes in adrenal status affect hypothalamic thyrotropin-releasing hormone gene expression in parallel with corticotropinreleasing hormone. *Endocrinology* 136:2795–802

- Kirsch T, Wellner M, Luft FC, Haller H, Lippoldt A (2001) Altered gene expression in cerebral capillaries of stroke-prone spontaneously hypertensive rats. *Brain Res* 910:106–15
- Kupprion C, Motamed K, Sage EH (1998) SPARC (BM-40, osteonectin) inhibits the mitogenic effect of vascular endothelial growth factor on microvascular endothelial cells. *J Biol Chem* 273:29635–40
- Mendis DB, Ivy GO, Brown IR (1998) SPARC/osteonectin mRNA is induced in blood vessels following injury to the adult rat cerebral cortex. Neurochem Res 23:1117–23
- Monaco HL (2000) The transthyretin-retinol-binding protein complex. *Biochim Biophys Acta* 1482:65–72
- Muller MB, Holsboer F (2006) Mice with mutations in the HPA-system as models for symptoms of depression. *Biol Psychiatry* 59:1104–15
- Muller MB, Landgraf R, Preil J, Sillaber I, Kresse AE, Keck ME, Zimmermann S, Holsboer F, Wurst W (2000) Selective activation of the hypothalamic vasopressinergic system in mice deficient for the corticotropin-releasing hormone receptor 1 is dependent on gluco-corticoids. *Endocrinology* 141:4262–9
- Musselman DL, Nemeroff CB (1996) Depression and endocrine disorders: focus on the thyroid and adrenal system. Br J Psychiatry Suppl 30:123–8
- Nemeroff CB, Widerlov E, Bissette G, Walleus H, Karlsson I, Eklund K, Kilts CD, Loosen PT, Vale W (1984) Elevated concentrations of CSF corticotropin-releasing factor-like immunoreactivity in depressed patients. *Science* 226:1342–4
- O'Shea PJ, Williams GR (2002) Insight into the physiological actions of thyroid hormone receptors from genetically modified mice. *J Endocrinol* 175:553–70
- Parkes DG, Weisinger RS, May CN (2001) Cardiovascular actions of CRH and urocortin: an update. *Peptides* 22:821–7
- Peeters PJ, Fierens FL, van den Wyngaert I, Goehlmann HW, Swagemakers SM, Kass SU, Langlois X, Pullan S, Stenzel-Poore MP, Steckler T (2004) Gene expression profiles highlight adaptive brain mechanisms in corticotropin releasing factor overexpressing mice. *Brain* Res Mol Brain Res 129:135–50
- Raines EW, Lane TF, Iruela-Arispe ML, Ross R, Sage EH (1992) The extracellular glycoprotein SPARC interacts with platelet-derived growth factor (PDGF)-AB and -BB and inhibits the binding of PDGF to its receptors. *Proc Natl Acad Sci USA* 89:1281–5
- Refojo D, Echenique C, Muller MB, Reul JM, Deussing JM, Wurst W, Sillaber I, Paez-Pereda M, Holsboer F, Arzt E (2005) Corticotropin-releasing hormone activates ERK1/2 MAPK in specific brain areas. *Proc Natl Acad Sci USA* 102:6183–8
- Reul JM, Holsboer F (2002) Corticotropin-releasing factor receptors 1 and 2 in anxiety and depression. *Curr Opin Pharmacol* 2:23–33
- Reul JM, Pearce PT, Funder JW, Krozowski ZS (1989) Type I and type II corticosteroid receptor gene expression in the rat: effect of adrenalectomy and dexamethasone administration. *Mol Endocrinol* 3:1674–80
- Roux KJ, Amici SA, Notterpek L (2004) The temporospatial expression of peripheral myelin protein 22 at the developing blood—nerve and blood—brain barriers. *J Comp Neurol* 474:578—88
- Schnitzer J, Franke WW, Schachner M (1981) Immunocytochemical demonstration of vimentin in astrocytes and ependymal cells of developing and adult mouse nervous system. *J Cell Biol* 90:435–47

- JM Deussing et al
- Stenzel-Poore MP, Cameron VA, Vaughan J, Sawchenko PE, Vale W (1992) Development of Cushing's syndrome in corticotropin-releasing factor transgenic mice. Endocrinology 130:3378-86
- Stevens SL, Shaw TE, Dykhuizen E, Lessov NS, Hill JK, Wurst W, Stenzel-Poore MP (2003) Reduced cerebral injury in CRH-R1 deficient mice after focal ischemia: a potential link to microglia and atrocytes that express CRH-R1. J Cereb Blood Flow Metab 23:1151-9
- Timpl P, Spanagel R, Sillaber I, Kresse A, Reul JM, Stalla GK, Blanquet V, Steckler T, Holsboer F, Wurst W (1998) Impaired stress response and reduced anxiety in mice lacking a functional corticotropin-releasing hormone receptor 1. Nat Genet 19:162-6
- Tsigos C, Chrousos GP (2002) Hypothalamic-pituitaryadrenal axis, neuroendocrine factors and stress. J Psychosom Res 53:865-71

- van Gaalen MM, Stenzel-Poore MP, Holsboer F, Steckler T (2002) Effects of transgenic overproduction of CRH on anxiety-like behaviour. Eur J Neurosci 15:2007-15
- Vargas F, Moreno JM, Rodriguez-Gomez I, Wangensteen R, Osuna A, varez-Guerra M, Garcia-Estan J (2006) Vascular and renal function in experimental thyroid disorders. Eur J Endocrinol 154:197-212
- Vorbrodt AW, Lossinsky AS, Wisniewski HM (1986) Localization of alkaline phosphatase activity in endothelia of developing and mature mouse blood-brain barrier. Dev Neurosci 8:1-13
- Yang YH, Dudoit S, Luu P, Lin DM, Peng V, Ngai J, Speed TP (2002) Normalization for cDNA microarray data: a robust composite method addressing single and multiple slide systematic variation. Nucleic Acids Res

Supplementary Information accompanies the paper on the Journal of Cerebral Blood Flow & Metabolism website (http:// www.nature.com/jcbfm)